



Available online at www.sciencedirect.com



Journal of Marine Systems 65 (2007) 484–508

JOURNAL OF
MARINE
SYSTEMS

www.elsevier.com/locate/jmarsys

A Mean Dynamic Topography of the Mediterranean Sea computed from altimetric data, in-situ measurements and a general circulation model

M.-H. Rio^{a,*}, P.-M. Poulain^b, A. Pascual^c, E. Mauri^b, G. Larnicol^c, R. Santoleri^a

^a *Istituto di Scienze dell'Atmosfera e del Clima, Rome, Italy*

^b *Istituto Nazionale di Oceanografia e di Geofisica Sperimentale (OGS), Trieste, Italy*

^c *CLS, Space Oceanography Division, Toulouse, France*

Received 28 September 2004; accepted 15 February 2005

Available online 22 December 2006

Abstract

In the Mediterranean Sea, where the mean circulation is largely unknown and characterized by smaller scales and less intensity than in the open ocean, the interpretation of altimetric Sea Level Anomalies (SLA) is rather difficult. In the context of operational systems such as MFS (Mediterranean Forecasting System) or MERCATOR, that assimilate the altimetric information, the estimation of a realistic Mean Dynamic Topography (MDT) consistent with altimetric SLA to be used to reconstruct absolute sea level is a crucial issue. A method is developed here to estimate the required MDT combining oceanic observations as altimetric and in-situ measurements and outputs from an ocean general circulation model (OGCM).

In a first step, the average over the 1993–1999 period of dynamic topography outputs from MFS OGCM provides a first guess for the computation of the MDT. Then, in a second step, drifting buoy velocities and altimetric data are combined using a synthetic method to obtain local estimates of the mean geostrophic circulation which are then used to improve the first guess through an inverse technique and map the MDT field (hereafter the Synthetic Mean Dynamic Topography or SMDT) on a 1/8° resolution grid.

Many interesting current patterns and cyclonic/anticyclonic structures are visible on the SMDT obtained. The main Mediterranean coastal currents are well marked (as the Algerian Current or the Liguro–Provençal–Catalan Current). East of the Sicily channel, the Atlantic Ionian Stream divides into several main branches crossing the Ionian Sea at various latitudes before joining at 19°E into a unique Mid-Mediterranean Jet. Also, strong signatures of the main Mediterranean eddies are obtained (as for instance the Alboran gyre, the Pelops, Ierapetra, Mersa-Matruh or Shikmona anticyclones and the Cretan, Rhodes or West Cyprus cyclones). Independent in-situ measurements from Sea Campaigns NORBAL in the North Balearic Sea and the North Tyrrhenian Sea and SYMPLEX in the Sicily channel are used to validate locally the SMDT: deduced absolute altimetric dynamic topography compares well with in-situ observations. Finally, the SMDT is used to compute absolute altimetric maps in the Alboran Sea and the Algerian Current. The use of absolute altimetric signal allows to accurately follow the formation and propagation of cyclonic and anticyclonic eddies in both areas.

© 2006 Elsevier B.V. All rights reserved.

Keywords: Mediterranean Sea; Altimetry; Mean Dynamic Topography

1. Introduction

* Corresponding author.

E-mail address: MH.rio@isac.cnr.it (M.-H. Rio).

In the last decade, the use of altimetric measurements from TOPEX/POSEIDON and ERS1,2 led to an

improved understanding of the Mediterranean sea level variability (Larnicol et al., 1995; Ayoub et al., 1998; Iudicone et al., 1998; Larnicol et al., 2002). This is despite the difficulty to capture the full mesoscale variability of the Mediterranean circulation due to its small dimensions (30–100 km) compared to the resolution permitted by the use of altimetric data. Furthermore, the lack of an accurate knowledge of the Mediterranean Mean Dynamic Topography (MDT) makes the variability as measured by altimetry particularly difficult to interpret. A positive anomaly detected by altimetry can indifferently be interpreted as the creation of an anticyclonic eddy, the strengthen (resp. the decay) of a quasi-permanent anticyclonic (resp. cyclonic) eddy or meander, the meandering or the spatial shift of a current. The Mediterranean circulation is characterized by numerous structures which were first identified punctually during in-situ measurements campaigns and whose permanent, recurrent or transient nature is, for some of them, still poorly known. An exhaustive inventory of the main Mediterranean features from basin scale to mesoscale, mainly based on the analysis of Sea Surface Temperature (SST) images, is given in Millot (1999) for the western Mediterranean basin and in Hamad et al. (2005) for the eastern basin. Despite the fact that a correlation exists between the dynamic height and the surface temperature, such images are not always easy to interpret as they only contain surface information and therefore do not reflect the ocean dynamic. The accurate knowledge of the Mediterranean MDT should help to correctly interpret the altimetric measurements and therefore to remove many remaining ambiguities on the Mediterranean variability. Moreover, the use of an accurate MDT was shown to contribute to major improvements in data assimilating forecasting systems (Le Provost et al., 1999; Le Traon et al., 2002). In the framework of operational systems as MERCATOR (France) and MFS (Mediterranean Forecasting System, Italy), which assimilate altimetric data into a general circulation model, the need of an accurate Mediterranean MDT becomes even more crucial. The scope of this study is to produce a tool allowing to compute the absolute sea level of the Mediterranean Sea (and the corresponding absolute geostrophic circulation) from altimetric measurements. The time period that has to be covered by the Mean Dynamic Topography thus shall correspond exactly to the time period used to compute Sea Level Anomalies from altimetric measurements using the conventional repeat track analysis. In order to be consistent with the SLA distributed by AVISO, which are computed at CLS relative to a seven year (1993–1999) mean profile, we compute here the Mediterranean Mean Dynamic Topography for the period 1993–1999. Section

2 describes the method and data used for the computation of the MDT. The core idea is the combination of altimetric anomalies and in-situ drifting buoy velocity measurements through a so called “synthetic method”, in order to obtain “synthetic estimates” of the MDT. This was already done globally by Niiler et al. (2003) and Rio and Hernandez (2004). The computation of a Mediterranean dataset of synthetic estimates of the MDT is done in Section 3. In Section 4, the Mediterranean MDT is mapped on a global 1/8th degree regular grid. (We will call Synthetic Mean Dynamic Topography, or SMDT, the MDT obtained through the synthetic method). The mean fields (dynamic height and geostrophic circulation) are first described qualitatively and a quantitative validation is successively done in three different areas where independent in-situ measurements are available. Before drawing the main conclusions of this work (Section 4), Section 5 presents some illustrations of using the Mediterranean SMDT to better follow the formation and propagation of eddies from altimetry in the Alboran Sea and along the Algerian Current path.

2. Methods and data

2.1. Method

The method used to compute a global Synthetic Mean Dynamic Topography of the Mediterranean Sea was already described and applied for the global ocean in Rio and Hernandez (2004). The main steps are explained briefly hereafter: the method is first based on a synthetic technique which consists in subtracting the oceanic variability as measured by altimetry to in-situ measurements of the absolute oceanographic signal in order to compute local estimates of the Mediterranean Mean Dynamic Topography (that we will refer to hereafter as ‘synthetic estimates’ of the MDT). The oceanographic signal can be the dynamic topography h but also any variable linearly related to it (as the geostrophic velocity (u_g, v_g)). Subtracting the altimetric Sea Level Anomaly h'_a (resp. the altimetric geostrophic velocity anomaly u'_a, v'_a), a synthetic estimate of the Mean Dynamic Topography $\langle h \rangle_s$ (resp. of the mean geostrophic circulation $\langle u \rangle_s, \langle v \rangle_s$) is obtained (Eqs. (1.1)–(1.3)).

$$\langle h \rangle_s = h - h'_a \quad (1.1)$$

$$\langle u \rangle_s = u_g - u'_a \quad (1.2)$$

$$\langle v \rangle_s = v_g - v'_a \quad (1.3)$$

This technique allows to get rid of the temporal variability contained in the in-situ observations. To

apply it properly, the in-situ data available first have to be processed in order to achieve consistency with the altimetric signal (see paragraph 3.1). Also, the altimetric anomalies have to be interpolated at the time and position of the in-situ data. Then the synthetic estimates obtained and the associated errors (including the error on the in-situ data measurements and processing as well as the error on the altimetric measurement and interpolation) are used to correct a first guess of the mean field (see paragraph 2.2.3) and map the Mean Dynamic Topography (and the corresponding mean geostrophic circulation) on a regular grid of the whole Mediterranean basin using a multivariate objective analysis (Bretherton et al., 1976; Le Traon and Hernandez, 1992).

The role of the first guess is twofold: first, the synthetic method provides estimates of the mean field only where in-situ measurements are available so that large parts of the Mediterranean Sea may remain unsampled (see paragraph 2.2). The first guess provides an estimate of the mean field in these areas. Second, the objective analysis can be applied properly only on zero mean fields. We use a remove–restore technique applying the multivariate objective analysis on the residuals between the synthetic observations and the first guess and then adding the first guess geostrophic velocity and dynamic topography to the estimated residual fields in order to recover the full mean dynamic signal.

2.2. Data

2.2.1. Drifting buoys

We used for this study the data of satellite-tracked surface drifters available in the Mediterranean Sea from 1 January 1993 to 11 November 1999 (Mauerhan, 2000; Poulain et al., 2004). Drifter of various types was

deployed during this period for scientific and operational purposes by various institutions from different countries. Drogue depth varied between 0 and 100 m, but the majority of the drifter data correspond to undrogued drifters measuring the currents in the first meter of water below the surface. The raw drifter data were first reduced and edited for spikes and outliers. They were then interpolated at uniformly distributed times using a kriging method (Hansen and Poulain, 1996), low-pass filtered (cut-off period 36 h) and subsampled at 6-h intervals. Velocities were computed by centered finite differences of the low-pass filtered positions. Details on the different drifters used and the processing applied can be found in Poulain et al. (2004).

The dataset obtained contains more than 120,000 velocity measurements whose spatial repartition in 1/8th boxes is given Fig. 1. The best sampled areas are the Adriatic and the Ionian Seas. No data are available in the Aegean Sea, the Northern Levantine basin and the Ligurian Sea. Errors on the processed buoy velocities due to wind and wave effects do not exceed 2–3 cm/s (Poulain et al., 2004).

2.2.2. Altimetry

The altimetric data available for this study are Sea Surface Heights (SSH) from ERS1-2 and TOPEX/POSEIDON (TP) satellites for the period 1st January 1993 to 1st October 2002 and from Jason-1 (J1) and TP-tandem mission, ERS-2 and Geosat Follow-On (GFO) from October, 1st 2002 to June, 30th 2003. Usual altimetric corrections are applied (Le Traon and Ogor, 1998) so as to obtain Sea Surface Height measurements with a precision of 3–4 cm. Then, a conventional repeat track analysis is performed to extract from these SSH, Sea Level Anomaly (SLA) relative to a seven year mean profile (1993–1999). The along-track residuals obtained

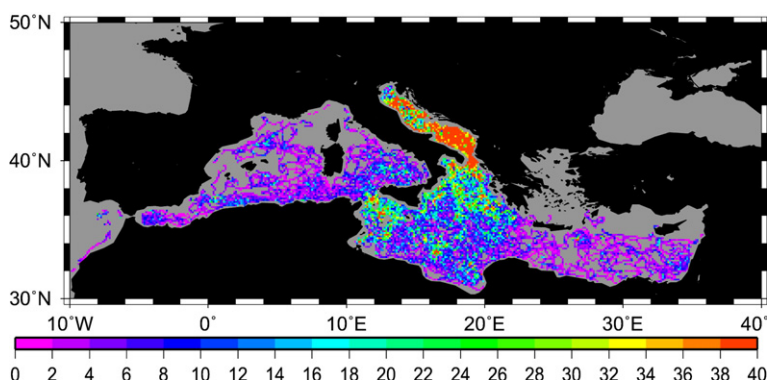


Fig. 1. Number of drifting buoy 6 hourly observations into 1/8th degree boxes for the period 1993–1999.

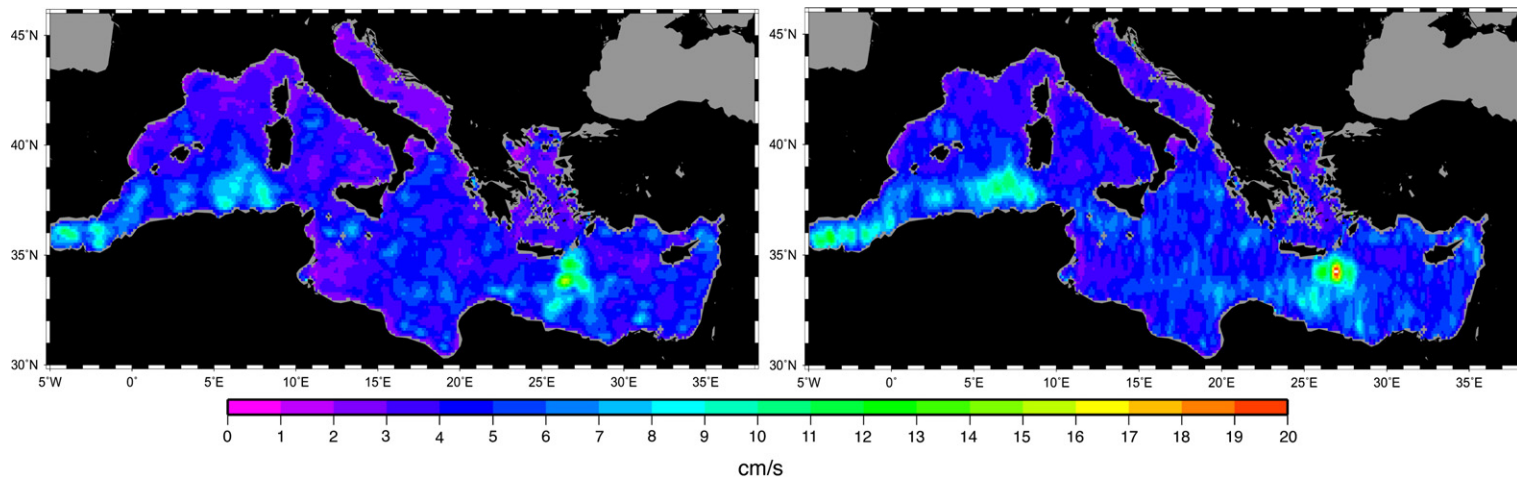


Fig. 2. Error on the zonal (left) and meridian (right) altimetric velocity anomaly.

are then filtered (40 km distance cut-off), sampled (1 point over 3 is conserved) and combined in order to compute weekly maps of SLA on a 1/8° regular grid using an objective analysis technique (Le Traon et al., 1998). The space and time correlation radius used for the mapping were chosen equal respectively to 100 km and 10 days (Pujol et al., 2004). Corresponding maps of geostrophic velocity anomalies are then computed from SLA maps by simple differentiation between adjacent grid points. Errors on the interpolated velocities are close to 30–40% of the signal variance (Pascual et al., 2007-this issue), with an interpolation of the meridional component less accurate than the zonal component by 10%–20% (Le Traon and Dibarboure, 1999). Fig. 2 shows the error estimated for the zonal and meridional components using the velocity variance computed from altimetric maps for the period 1993–1999. Error on the zonal (resp. meridional) component was chosen equal to 30% (resp. 40%) of the signal variance. Errors greater than 15 cm/s are obtained on both velocity components southeast of Crete, in the formation area of the Ierapetra cyclone. Errors of the order of 10 cm/s are associated to the Alboran Sea and the Algerian Current. In the Adriatic Sea, the North Balearic Sea, the southwest Ionian Sea, errors are less than 5 cm/s.

2.2.3. First guess

The first guess used in this study is the average over the period 1993–1999 of outputs from the MFSTEP (Mediterranean Forecasting System: Toward Environmental Predictions) model (Demirov et al., 2003). This model is based upon the Modular Ocean Model code (MOM1.0). Its resolution is 1/8th degree with 31 levels unevenly spaced in the vertical. Its equations consider the rigid-lid approximation. The 1993–1999 mean field

used issues from a run with no data assimilation. It features two strong cyclonic gyres in the Northern part of the Western Mediterranean basin and all around the Levantine Sea (Fig. 3). In the Western basin, the mean Algerian Current is not along the African coasts but further North. Passing the Sicily channel, two main mean paths are visible. The first one is along the Tunisian and Libyan coasts while the second one crosses the central part of the Ionian basin, toward the Levantine Sea. The MFSTEP mean misses the northern part of the Adriatic Sea, north of 43°N, so that we arbitrarily completed it with a flat surface. This should have no influence on the results since many observations are available in that area (Fig. 1).

3. Construction of a set of synthetic estimates

3.1. Processing of the drifting buoy velocities

Before subtracting the ocean variability as measured from altimetry from the drifting buoy velocities, the latter have to be processed in order to achieve consistency with the altimetric signal. Drifting buoys velocities contain both the geostrophic and the ageostrophic component of the ocean circulation. Provided the ageostrophic part is removed, they can be linearly related, through geostrophy, to the ocean dynamic topography. The 36 h filtering allows to remove some ageostrophic current components such as tidal currents, inertial oscillations (the inertial period varies between 16.4 h at latitude 47°N and 23.9 h at latitude 30°N) and other high frequency ageostrophic phenomena (Stoke's drift, internal waves). In addition, the ageostrophic component due to Ekman currents has to be estimated and removed. We use a model by Mauri and Poulain

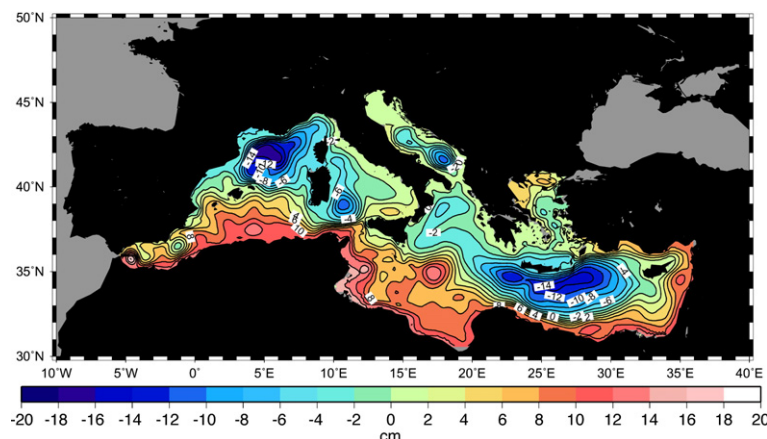


Fig. 3. Mean Dynamic Topography issued from the average over the period 1993–1999 of MFSTEP model outputs.

(2004) in which the Ekman current is directed at 23.22° on the right of the wind direction and has an amplitude equal to 1.07 time the wind velocity amplitude. Wind velocities from the ECMWF (European Center for Medium-range Weather Forecasts) 40-year re-analysis are used. This model was found to explain 7.86% of the variance of the drifting buoy dataset used. The model was optimized only for buoys with a drogue centered in the first meters of water for the period 1995–1999. This corresponds to nearly 70% of the total number of velocity measurements, located mainly in the Adriatic and the Ionian Seas. In this study, we corrected for the Ekman component only for the drifting buoys for which the model was optimized so that part of our dataset (~30%) still contains an ageostrophic component due to Ekman currents. The removal of the Ekman component results in a reduction of the Eddy Kinetic Energy (EKE) computed into 1/8th boxes from the drifting buoy velocity dataset in 75% of the cases. We computed the ratio between the drifting buoy EKE after and before the removal of the Ekman component (see histogram Fig. 4). In 60% of the boxes, the Ekman component accounts for less than 30% of the total EKE (On Fig. 4: ratio between 0.7 and 1).

3.2. Consistency between processed drifting buoy velocities and altimetric data

In order to check the consistency between the geostrophic in-situ velocities extracted from the drifting buoy data and the altimetric velocity anomalies, we compare the EKE computed in 1/8th boxes from the processed in-situ velocities and the altimetric velocity anomalies interpolated at the buoy's time and position

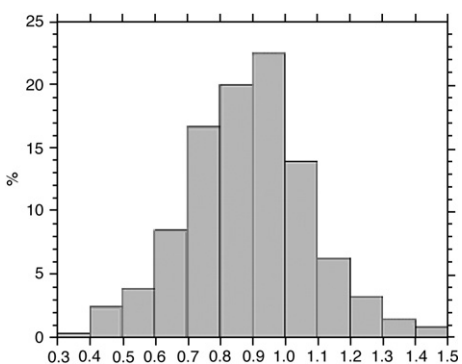


Fig. 4. Histogram (in percent of boxes) of the ratio between the EKE computed from drifting buoy velocities after and before the removal of the Ekman component. A ratio lower than 1 means that the removal of the Ekman component results in a decrease of the drifting buoys EKE computed in 1/8th degree boxes.

from the altimetric velocity anomaly maps (2.2). Results are shown Fig. 5. EKE values deduced from the drifting buoy velocities (Fig. 5a) are similar to those obtained by Mauerhan (2000), Poulain (2001, in preparation), Poulain and Zambianchi (in press), Salas et al. (2001) using the same dataset without the removal of the Ekman current. In our study, only part of the drifting buoys of the Adriatic and Ionian Sea have been corrected for the Ekman component so that results between the various studies do not differ substantially. The highest values (more than $400 \text{ cm}^2/\text{s}^2$) are obtained in the Alboran Sea, along the Algerian Current path and at the entrance of the Sardinia channel, where anticyclonic eddies originated from the meandering of the Algerian Current are known to be blocked by topography before propagating back westward into the central western Mediterranean basin (Millot, 1985). In the eastern basin, values higher than $300 \text{ cm}^2/\text{s}^2$ are found southwest of Peloponese and southeast of Crete. Both cases correspond to areas where anticyclonic eddies (respectively the Pelops and the Ierapetra anticyclones) are known to form regularly (Theocharis et al., 1993; Theocharis et al., 1999). EKE greater than $200 \text{ cm}^2/\text{s}^2$ is found in the Sicily channel and the northern part of the Ionian basin as well as along the Israeli coast. Homogeneous values, close to $60–80 \text{ cm}^2/\text{s}^2$, are found in the interior of the Adriatic Sea with higher values along the coasts ($120–140 \text{ cm}^2/\text{s}^2$). Values close to $60–80 \text{ cm}^2/\text{s}^2$ are also found in the southern Tyrrhenian Sea. The southern part of the Ionian Sea is characterized by EKE values ranging from 60 to $150 \text{ cm}^2/\text{s}^2$. In all remaining areas (mainly Balearic and Levantine Sea), values are weak, less than $30 \text{ cm}^2/\text{s}^2$. However, only few data are available and the results obtained might not be representative of the actual EKE level of these regions.

For comparison, the EKE values obtained from altimetry are displayed in Fig. 5b. They are similar to values already obtained by Judicone et al. (1998) from two years of TOPEX POSEIDON data and Pujol and Larnicol (2005) from 11 years of T/P and ERS data. The first result is that the EKE maps deduced from altimetry feature the same patterns of high and low variability (strong signal in the Alboran Sea, the Algerian Current, the Ierapetra area, intermediate values in the Sicily channel and Ionian Sea, low values in the Adriatic and Tyrrhenian Seas...). However the levels of energy are very different, the altimetric EKE being inferior to the drifter EKE by a factor of up to 2 or 3: values up to $200–300 \text{ cm}^2/\text{s}^2$ are obtained southwest of Sardinia and in the Ierapetra region. The EKE in the Alboran Sea and the Algerian Current ranges between 80 and $120 \text{ cm}^2/\text{s}^2$. In

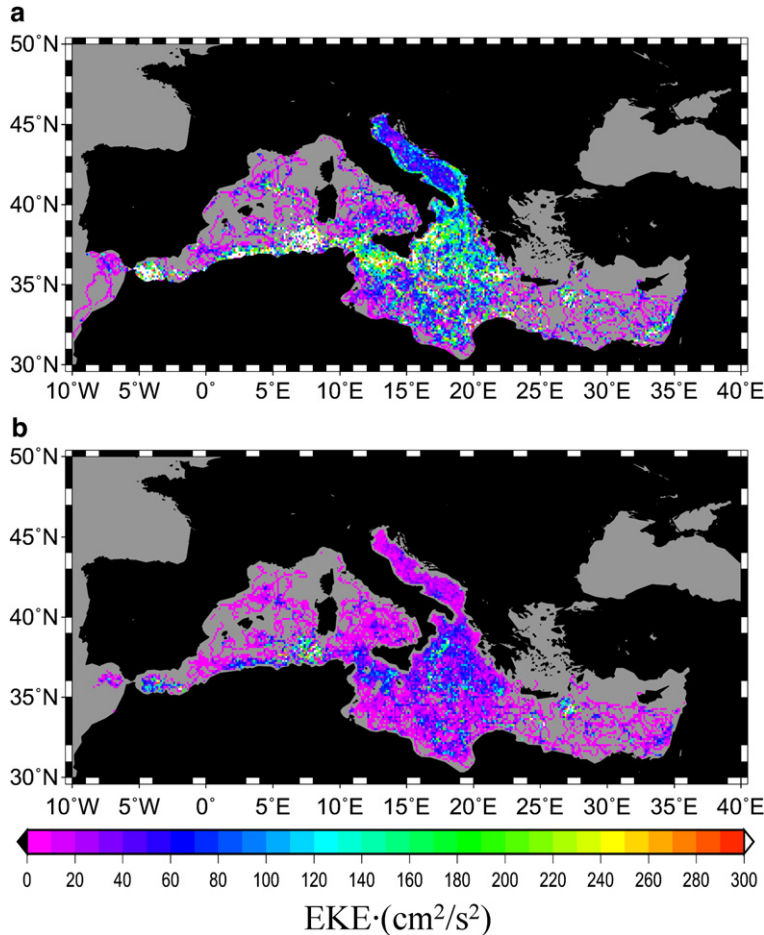


Fig. 5. Eddy Kinetic Energy computed from: a—the total dataset of drifting buoy velocity measurements filtered at 36 h and corrected for the Ekman component in the Ionian and Adriatic seas, b—altimetric velocity anomalies computed from SLA maps and interpolated at the buoy's time and position.

the Adriatic Sea and the Tyrrhenian Sea values are less than $50 \text{ cm}^2/\text{s}^2$.

This discrepancy is partly explained by the errors on both datasets. Some of the drifting buoy velocities still contain an ageostrophic component due to Ekman currents. However, as drawn in (3.1) it should account only up to 25% of the total EKE. Also, the Lagrangian character of the drifting buoys, which tend to gather in convergence areas (Davis, 1998) will lead to an overestimation of the EKE in high variability areas. Errors on the interpolation of the altimetric anomalies may also account for the discrepancy (errors up to 30% of the altimetric variability, see 2.2). However, the main source of discrepancy comes from the diverse sampling capability of both data type. This factor is crucial in the Mediterranean Sea where the typical dimensions of the mesoscale (30–100 km) are inferior to altimetric inter tracks (240 km for TP at 40°N). Altimetric anomalies interpolated along an eddy path will miss a part of the

eddy variability whereas a drifting buoy following the same eddy trajectory will measure the mean circulation added to the whole eddy variability. The combination of several satellites is crucial to increase the resolution of altimetric data and thus the description of the Mediterranean mesoscale. For instance, Pascual et al. (2007-this issue) have shown that in average, the merged Jason-1 + ERS-2 + T/P + GFO maps yield EKE levels 15% higher than Jason-1 + ERS-2. Unfortunately, the configuration with 4 satellites is only available since October 2002.

3.3. Method efficiency

Once the drifting buoy velocities have been processed, synthetic mean velocities ($\langle u \rangle_s, \langle v \rangle_s$) can be computed (Eqs. (1.2) and (1.3)). A direct consequence of the discrepancies highlighted in 2.2 between the in-situ geostrophic velocities and the altimetric velocity anomalies is that not the total ocean temporal variability

is removed from the drifting buoys geostrophic velocities when applying the synthetic method, as it ideally should. The synthetic mean velocity dataset contains a residual temporal variability (as computed in 1/8th boxes) that accounts for the errors on the altimetric and drifting buoy datasets as well as for their different sampling capabilities. The variance of the synthetic mean velocities in 1/8th boxes is the sum of this temporal residual variance and the spatial variance of the Mediterranean 1993–1999 mean geostrophic circulation as computed in 1/8th boxes (that we assume is small, i.e. we assume that the spatial scales of the Mediterranean 1993–1999 mean geostrophic circulation are greater than 1/8th). In any case, for the synthetic method to be efficient, the variance of the synthetic mean velocities in 1/8th boxes should be inferior to the variance computed from the initial in-situ geostrophic velocities (i.e. before subtracting the altimetric anomaly). Fig. 6 (top) shows the ratio between the variance of the synthetic estimates and the variance of the in-situ geostrophic velocities. Variance is reduced (i.e. the ratio obtained is lower than 1) in 70% of the boxes for the zonal component and 65% for the meridional compo-

ment. Ratio greater than 1 are observed in the Adriatic Sea. In this area, which is mainly coastal, altimetric measurements are known to be less accurate. In particular, tidal models used for altimetric correction are not satisfactory.

In order to remove from our datasets altimetric or drifting buoys data with too large errors, we now select the data used to compute synthetic mean velocities through the following method: we consider all 1/8th boxes in which the variance of both the zonal and meridional component of the synthetic mean velocities is greater than the initial in-situ geostrophic velocity variance. This corresponds to 26% of the total 1/8th boxes. For each box, we compute the mean value and standard deviation of the zonal and meridional synthetic mean velocities and remove the synthetic mean velocities whose difference to the mean value is greater than the box standard deviation for at least one component. This selection removes 9% of the total number of synthetic velocities, mostly located in the Adriatic Sea. As illustrated in Fig. 6 (bottom) it allows to improve the synthetic method efficiency in most areas. The ratio between the variance computed from synthetic

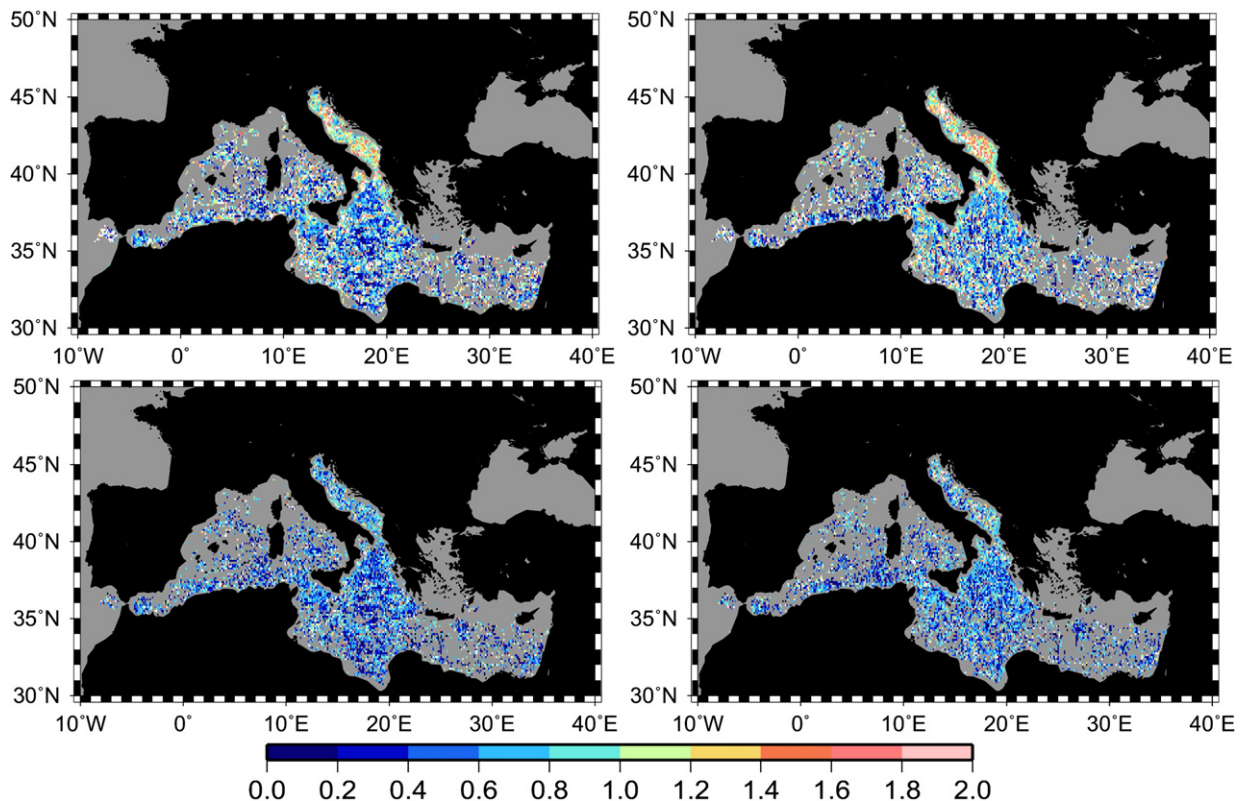


Fig. 6. Ratio between the ocean variability computed from the synthetic velocities and the initial velocities for the zonal (left) and the meridian (right) components before (top) and after (bottom) selection of the data.

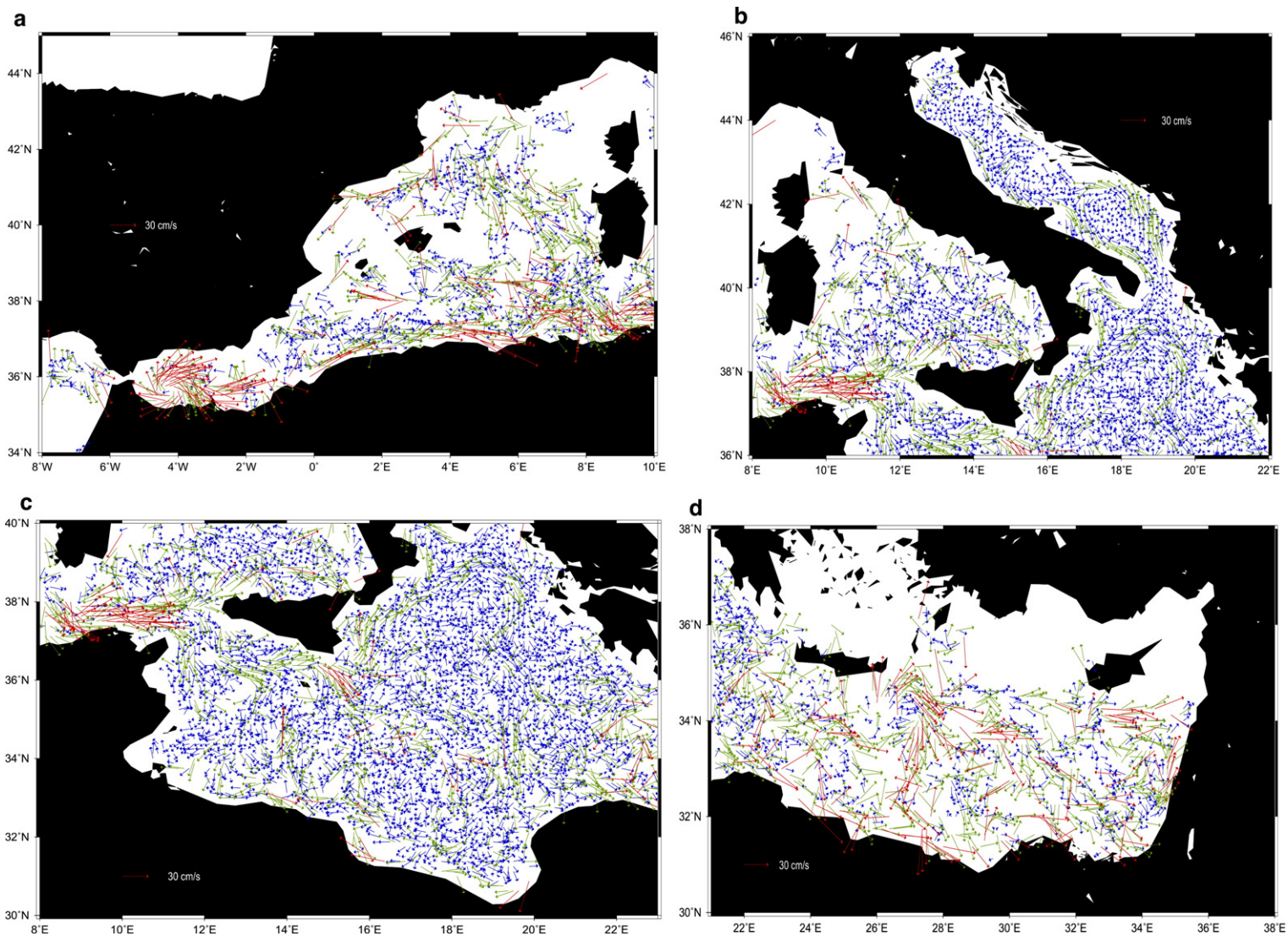


Fig. 7. Synthetic velocities obtained from the combination of altimetric data and drifting buoy measurements as described in this paper. Regions considered are a—the Alboran–Algerian–Balearic area b—the Tyrrhenian and Adriatic Seas c—the Ionian Sea and d—the Levantin basin. Velocities greater than 15 cm/s (resp. 30 cm/s) are displayed as green (resp. red) arrows. (For interpretation of the references to color in this figure legend, the reader is referred to the web version of this article.)

mean velocities and initial geostrophic velocities is now lower than 1 in 90% of the boxes for both components of the velocity.

3.4. Set of synthetic mean velocities

As discussed in Section 3.2.3, the synthetic mean velocity obtained subtracting the altimetric velocity anomaly interpolated from the altimetric velocity maps from the buoy geostrophic velocity thus contains a residual ocean temporal variability. In order to reduce this error, we average the obtained synthetic mean velocities into 1/8th boxes and consider these box means as final synthetic estimates. (We will now call synthetic estimates these 1/8th box means). The obtained mean velocities are displayed in Fig. 7 for four sub-basins of the Mediterranean Sea (the Alboran–Algerian–Balearic area, the Tyrrhenian and Adriatic Seas, the Ionian Sea and the Levantine Sea). Red arrows correspond to mean velocities greater than 30 cm/s. They are found in the Alboran Sea, in the Algerian Current and in the Levantin basin (along the African coasts and South of Crest and Rhodes islands). An error is associated to each estimate equal to the box variance divided by the number of independent observations available. In a same box, two velocities are considered independent if measured by a different buoy or, for a same buoy, if measured with more than 3 days interval. The choice of 3 days was done considering the Lagrangian time scales measured in the Mediterranean Sea (Mauerhan, 2000).

4. The Mediterranean Synthetic Mean Dynamic Topography (SMDT)

We use the synthetic estimates computed in the previous section to map the Mediterranean SMDT on a

1/8° regular grid using a multivariate analysis based on a remove restore technique as described in 2.1. The space correlation radius used for the inversion are computed from the residual observations (i.e. synthetic estimates minus first guess) and found equal to 50 km both for the zonal and meridional components of the velocity. We chose to consider for inversion all residual observations contained in a 150 km radius sphere of influence around the point to estimate. A crucial point here is that, although we use outputs from a general circulation model as first guess, the synthetic mean field obtained in areas covered by drifting buoy velocities is strictly an observed mean field whose accuracy is directly linked to the number of observations used for the estimation (see Fig. 1—the smallest errors will be found for instance in the Ionian and Adriatic Seas while stronger errors will characterize areas like the Balearic Sea or the Levantine basin). Inversely, where no observations are available (mainly the northern Levantine Sea), the first guess is obtained (whose accuracy is linked to the MFSTEP model errors).

The SMDT obtained is displayed in Figs. 8–11. We superimposed as blue arrows the mean geostrophic circulation also obtained as output of the multivariate objective analysis. In the next two sections the SMDT is first described focussing on four different sub-basins (4.1) and then validated using independent observations (4.2).

4.1. Qualitative description

The following paragraphs propose a description of the Mediterranean Synthetic MDT and the corresponding mean geostrophic circulation estimated through the method detailed previously. Beforehand, we want to remind clearly what was already stated in introduction:

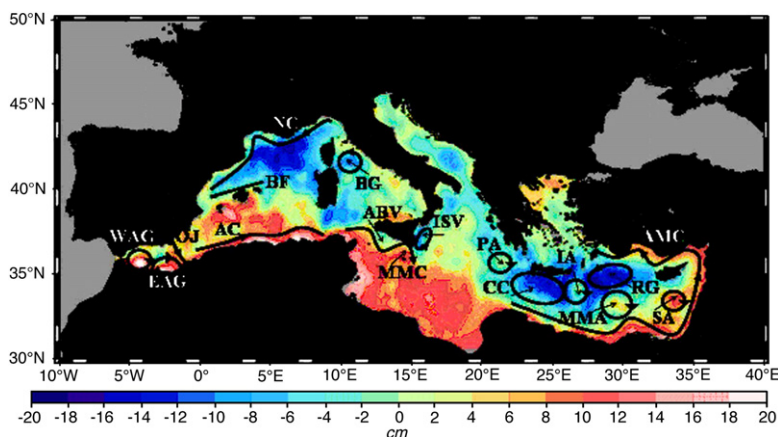


Fig. 8. Main features visible on the Synthetic Mean Dynamic Topography computed in this paper.

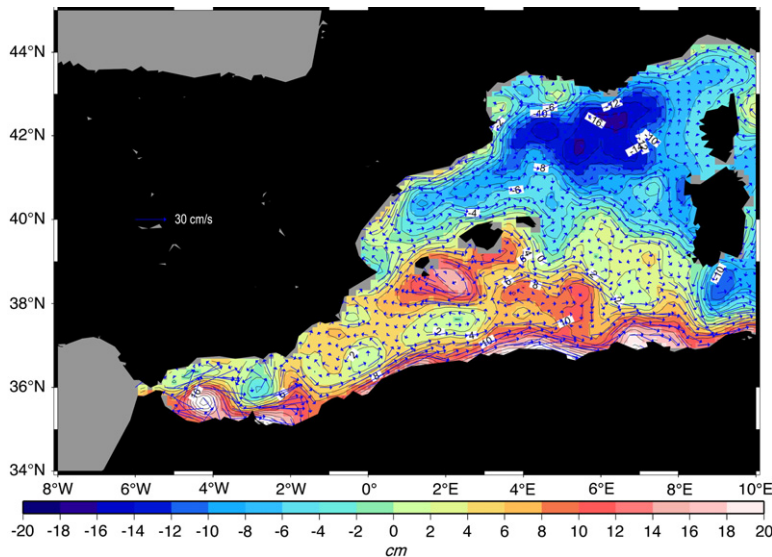


Fig. 9. Synthetic Mean Dynamic Topography in the Alboran–Algerian–Baleares area. The corresponding mean currents are superimposed as blue arrows. (For interpretation of the references to color in this figure legend, the reader is referred to the web version of this article.)

The MDT obtained here and described hereafter is a tool designed to compute absolute sea level and geostrophic velocities from altimetry. Many authors have in the past proposed various schemes for the general circulation of the surface Atlantic Water in the Mediterranean Sea (Nielsen, 1912; Ovchinnikov, 1966; Lacombe and Tchernia, 1972; Robinson et al., 1991; Robinson and Golnaraghi, 1993; Millot, 1999; Hamad et al., 2005). The purpose here is not to propose a new schematic of the Mediterranean general circulation but rather to

describe the very specific mean obtained, for the period 1993–1999, of the Mediterranean dynamic topography whose combination with altimetric Sea Level Anomalies will help to better interpret the altimetric signal and highlight the stationary/recurrent/transient nature of known structures as well as the different paths taken by the Mediterranean surface water throughout the basin. For the purpose of clarity, all main features of the mean circulation discussed hereafter have been schematically reproduced on Fig. 8.

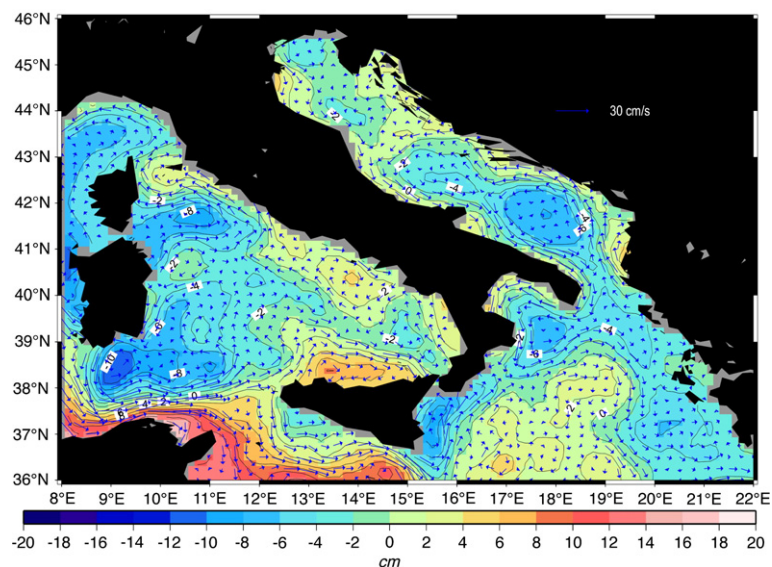


Fig. 10. Synthetic Mean Dynamic Topography in the Tyrrhenian and Adriatic seas. The corresponding mean currents are superimposed as blue arrows. (For interpretation of the references to color in this figure legend, the reader is referred to the web version of this article.)

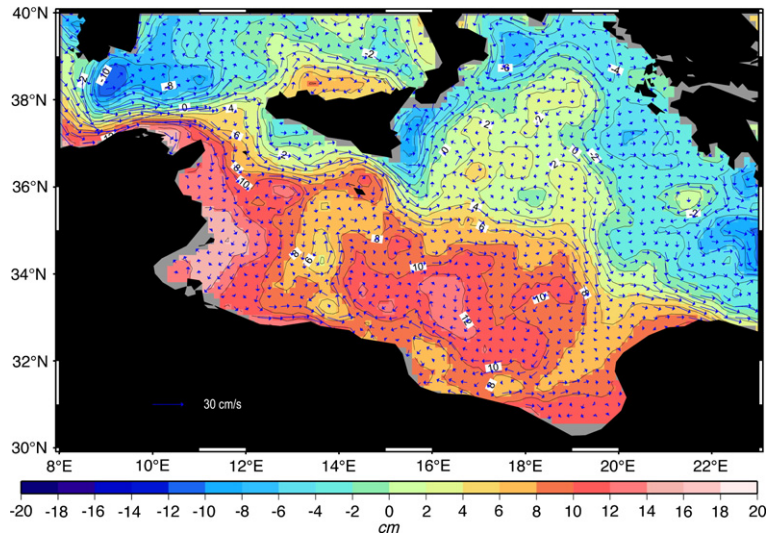


Fig. 11. Synthetic Mean Dynamic Topography in the Ionian Sea. The corresponding mean currents are superimposed as blue arrows. (For interpretation of the references to color in this figure legend, the reader is referred to the web version of this article.)

4.1.1. The Alboran–Algerian–Baleares area (Fig. 9)

East of Gibraltar, the synthetic mean field features a strong signature of the anticyclonic Western Alboran Gyre (WAG), with mean velocities ranging from 20 to 30 cm/s. A second anticyclonic gyre, the Eastern Alboran Gyre (EAG) is known to be generated in the eastern part of the Alboran Sea, anticyclonic most of the time but more variable than its western counterpart. On average over the 1993–1999 period, only a large anticyclonic meander centered at 2°W is visible. Northeast of it, joining Spain to Algeria, mean velocities of 10 cm/s are associated to the Almeria–Oran jet (AOJ). West of it, centered at 3°E 36°N, the SMDT features a cyclonic structure that might be the signature of small cyclonic eddies which were described to be generated in the area by Davies et al. (1993), Tintore et al. (1991, 1994). Further east, contrary to what is obtained in the first guess (Fig. 3), the mean Algerian Current (AC) is clearly located along the Algerian coasts. A very thin, straight and intense mean jet, with velocities exceeding 30 cm/s, is obtained between 1°W and 1°E. Then the width of the mean current increases. Two cyclonic recirculation cells are visible centered at 0.25°W and 2.25°E. The Algerian Current is known to develop large meanders giving rise to anticyclonic eddies that are blocked at the level of the Sardinia channel and propagate westward (Font et al., 1998; Salas et al., 2001). The meandering path of the mean current east of 1°E as well as the many anticyclonic structures visible in Fig. 9 on the northern side of the Algerian Current are a clear signature of this activity.

The northern part of the basin is fully occupied by a strong mean cyclonic circulation. Its northern and eastern side corresponds to a well marked mean Northern Current (NC, Millot, 1991; Font et al., 1998) all along the Italian, French and Spanish coasts from 10°E to 0°. On the SMDT, this current features mean velocities ranging between 10 and 15 cm/s. A strong mean current, directed north eastward, is also visible North of the Balearic islands and corresponds to the North Balearic front (NBF). It separates the overall anticyclonic mean circulation of the southern part of the basin from the northern, overall cyclonic, mean circulation.

The Ligurian Sea features, in the South, a north-eastward current along Corsica and, in the North, a westward current along the French and Italian coasts. The Northern and Eastern sides of Corsica are not sampled by observations (Fig. 1); the mean circulation obtained in these areas corresponds to the first guess circulation.

4.1.2. The Tyrrhenian and Adriatic Seas (Fig. 10)

The synthetic mean circulation in the Tyrrhenian Sea is overall cyclonic along the Sicilian, Italian, Corsican and Sardinian coasts, with three anticyclonic recirculation cells located on the northern side of Sicily (centered at 14°E 39°N), off Naples (centered at 14°E 41.5°N) and between the Elba island and Corsica (10.5°E 42.5°N). Centered at 10.75°E 41.75°N, the SMDT presents a clear signature of the Bonifacio gyre (BG) which is known to be a semipermanent cyclonic

structure in the area generated by the interaction of westerly winds with the orography of Sardinia and Corsica (Artale et al., 1994). In this process an anticyclonic gyre is also generated to the south but dissipates more quickly so that its signature on the Synthetic MDT (centered at 10.5°E 40.5°N) is weaker than its cyclonic counterpart. A strong cyclonic mean structure is also obtained south of Sardinia, centered at 9°E 38.5°N. East of the Sardinia channel, the current follows two main mean paths. One is eastward into the Tyrrhenian Sea and the other one is south-eastward, into the Ionian basin, through the Sicily channel.

The synthetic Mean Dynamic Topography in the Adriatic Sea is composed of three main anticyclonic patterns, centered respectively at 18°E 42°N, 16°E 43°N, and 15°E 44.5°N. The mean circulation around these patterns is anticlockwise all around the basin, northwestward along the Albanian and Croatian coasts and southeastward along the Italian coasts (Artegiani et al., 1997; Poulain, 2001).

4.1.3. The Ionian Sea (Fig. 11)

The Ionian Sea, apart from its southern extremity, along the African coasts, where only few observations are available, is an area well sampled by the drifting buoys dataset (Fig. 1). Entering the Ionian basin, the mean current divides into two distinct branches (Fig. 11). The first branch is directed southward, not along the Tunisian coasts but further east, along the continental slope, in good agreement with Hamad et al. (2005). At the level of the Libyan coast, at 12°E, it turns east along the coast until 14°E. Further east, three cyclonic cells are visible along the coast, located at 14°E 33°N, 16°E 32°N, 17.5°E 31.5°N. However, conversely to what is seen in the first guess (Fig. 3), no continuous mean current eastward along the Libyan coast is obtained. This is in disagreement with Hamad et al. (2005) who identified this southern path as the main passage of Atlantic Water from the western Mediterranean basin to the Levantine Sea, analyzing SST images from 1993 to 2002.

The second branch of the mean flow at the level of the Sicily channel has a clear Northwest–South-eastward direction and features the signature of semi-permanent/recurrent structures already identified in the region by Robinson et al. (1999) and further observed by Lermusiaux and Robinson (2001): the cyclonic Adventure Bank Vortex (ABV) centered at 12.8°E 37.4°N, the anticyclonic Maltese Channel Crest (MCC) at 14.5°E 36.5°N and the cyclonic Ionian Shelfbreak Vortex (ISV) at 15.5°E 36.5°N. The latter feature could be the signature of the numerous instabilities generated

by the main flow in the area (Buongiorno Nardelli et al., 2001). The mean path of the current around these main structures is as follows (Fig. 11): It circulates eastward toward Sicily and describes a large anticyclonic meander centered at 11.9°E 37.5°N whose eastern side corresponds to the western part of the ABV. Then the path is eastward with mean velocities close to 15 cm/s. At around 13.2°E, as already observed in Mauerhan (2000), one part of the mean flow is directed South toward the African coast (with maximum mean velocities reaching 10 cm/s) while the main part veers North to form a large anticyclonic meander (the MCC) characterized by an increase of the mean flow velocities (up to 20 cm/s). South of Malta, the SMDT features a recirculation pattern that bifurcates southward from the main mean current at 14.8°E and extends westward along 35.6°N, with velocities ranging from 5 to 10 cm/s. East of Malta, in good agreement with previous observations by Lermusiaux (1999) and Buongiorno Nardelli et al. (2001), the mean current divides into two main branches that cross the entire Ionian basin toward the Levantine Sea and merge at 19°E. The first branch is in a south-eastward direction and crosses the basin with large meanders and mean velocities of the order of 10 cm/s. South of this main current, an overall mean clockwise circulation seems to dominate the southern Ionian basin. This path has been identified as the main route of the Atlantic Water entering the Ionian basin toward the Levantine Sea by many authors (Ovchinnikov, 1966; Lacombe and Tchernia, 1972; Robinson and Golnaraghi, 1993) but is absent from the analysis of Hamad et al. (2005) who consider that the central Ionian basin is mainly filled by anticyclonic eddies. The mean circulation computed here for the period 1993–1999 clearly features the signature of a main stream crossing the Ionian basin in its central part. The second branch is directed north-eastward until 19°E 39°N and then south-eastward toward the central Ionian Sea. This northern branch has been observed many times until 1998 (Poulain, 1998; Robinson et al., 1999), with a strong seasonal variability (Robinson and Golnaraghi (1993) argue it is mainly a summertime feature), and may have disappeared afterward (Manca et al., 2002). This northern path of the MAW has a clear signature on the SMDT computed here. This is partly in disagreement with the analysis of Hamad et al. (2005) in which the northern branch is said to stop at its northern extremity, without any continuity with the eastern part of the Ionian basin. Once again, we do not argue that these paths (the central and northern) have been followed continuously all through the period 1993–1999 by the surface Atlantic water but that they have occurred recurrently enough to have a signature on the mean field.

More precisely Pujol et al. (2004) and Poulain (*in preparation*) have shown that those two pathways rather correspond to two distinct states of the Mediterranean general circulation with a northern circulation before 1997, and a more intense circulation in the central Ionian basin after 1997. On average, both branches merge at 19°E, 34°N and enter the Levantine Sea as a unique and large stream at latitudes ranging between 32.5°N and 33.5°N. It is joined at 20°E by the weaker mean flow mentioned previously along the Libyan coasts. The mean flow along the Peloponnesian and the Greek coast is slightly north-westward into the Adriatic Sea. A stronger mean current is obtained from the Adriatic Sea south-westward into the Ionian Sea along the Italian and Sicilian coasts. Between this path and the previously mentioned north-eastward flow, the SMDT features the signature of two cyclonic circulation patterns, the first one centered at 15.5°E and 37°N and the second one at 18°E and 39°N.

Finally, the SMDT features a strong signature of the Pelops anticyclone (PA) at 21.5°E 35.5°N, with maximum mean velocities close to 10 cm/s. This gyre, which is known to be a recurrent feature most probably forced by the winds south of Peloponese (Le Vourch et al., 1992; Theocharis et al., 1999), was absent from the first guess (Fig. 3).

4.1.4. The Levantine Sea

In the Levantine Sea, the mean circulation derived from the SMDT is overall cyclonic all around the basin (Fig. 12). In the South, large meanders characterize the main mean stream along the Egyptian coast. Very close to the coast until 28°E, it then detaches slightly and the signature of small anticyclonic re-circulation cells are obtained between the main stream and the coast (at 29.8°E, 31°E, 32°E, 33°E). In the North, where no

synthetic observations were available, the SMDT is equivalent to the first guess (Fig. 3) that nevertheless relatively well represents the Asia Minor Current (AMC). In the central part of the basin, contrary to what is observed in the first guess, the SMDT features strong anticyclonic signatures in the Shikmona area (SA—centered at 33.8°E 33.5°N), the Mersa–Matruh area (MMA—double anticyclonic circulation cell centered at 29.5°E 33°N) and the Ierapetra formation area (IA—centered at 27°E, 34.3°N). The latter structure clearly separates, on its western side, the signature of the Cretan cyclone (CC—centered at 25°E 34°N) from the cyclonic signature, on its eastern side, of the Rhodes gyre (RG—centered at 28°E 34.5°N).

4.2. Quantitative validation

To validate the Synthetic Mean Dynamic Topography, we compare independent in-situ measurements (dynamic heights and drifting buoy velocities) with the corresponding altimetric absolute signal (computed interpolating the altimetric sea level – resp. velocity – anomaly to the position of the in-situ measurement and adding the SMDT – resp. the corresponding mean geostrophic velocity). Comparisons are done computing root mean square differences between the two datasets and regression slopes. Independent in-situ observations are available in four different areas: the North Balearic Sea (4.2.1), the Bonifacio gyre (4.2.2), the Sicily channel (4.2.3) and the Southern Adriatic Sea (4.2.4).

4.2.1. The North Balearic Sea

We used dynamic heights measured during the NORBAL-3, -4 and -5 campaigns (North Balearic Sea

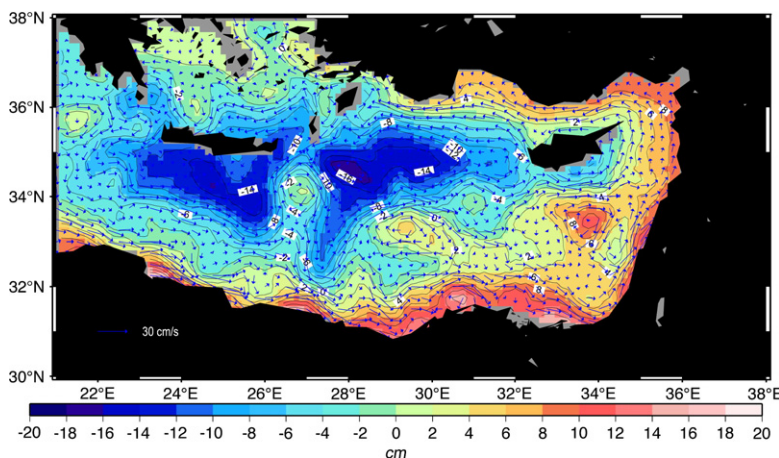


Fig. 12. Synthetic Mean Dynamic Topography in the Levantine Sea. The corresponding mean currents are superimposed as blue arrows. (For interpretation of the references to colour in this figure legend, the reader is referred to the web version of this article.)

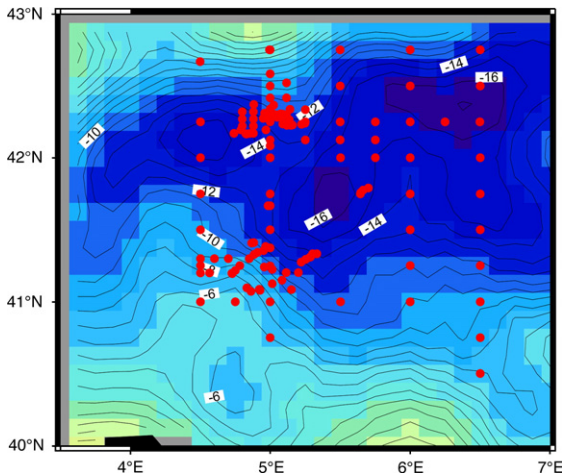


Fig. 13. The Synthetic Mean Dynamic Topography in the North Balearic Sea. The color scale is the same as for Fig. 8. Contours are every centimetre. Red circles correspond to the location of in-situ hydrologic profiles measured during the NORBAL campaigns. (For interpretation of the references to color in this figure legend, the reader is referred to the web version of this article.)

—2002, 2003). A total of 185 CTD profiles were available in the area, among which 57 profiles down to 2000 m, 64 profiles down to 1500 m, 68 profiles down to 1000 m and 155 profiles down to 500 m. We superimposed their location on the SMDT obtained in the area as red circles (Fig. 13). We use for that period altimetric anomalies computed combining data from four different satellites (see 2.2.2). We compare the absolute altimetric heights to the dynamic heights computed relative to the various profile depths. Results (regression slope and root mean square differences) are displayed Table 1 for the various depths and using to reference the altimetric anomalies either the SMDT or the first guess or a zero mean.

Independently from the mean used to compute absolute altimetric height, best comparison results (RMS in per-

centage of ocean altimetric variability) are obtained using dynamic heights relative to 1000 m to 2000 m in respect to the shallower 500 m depth. RMS differences between the two datasets contain the error on the mean used, the in-situ and altimetric measurement errors, the barotropic component of the ocean dynamic topography, contained in the altimetric signal but not in the in-situ dynamic height as well as the deep baroclinic component (deeper than the in-situ dynamic height reference depth) of the ocean dynamic topography. In all cases, regression results are improved when using the SMDT instead of the first guess to reference altimetric anomalies: the regression slope comes closer to one (1.08 considering the dynamic height relative to 1500 m, instead of 1.16 with the first guess and 0.92 with the zero mean) and the root mean square difference to observations is reduced (39.9% of the signal variance instead of 51.2% when using either the first guess or the zero mean).

4.2.2. The Bonifacio gyre

A total of 16 hydrological profiles were measured during the NORBAL-2 campaign east of the Bonifacio channel, between the 7th December 2001 and 11th December 2001, in an area where westerly winds recurrently interact with the Corsica and Sardaigna orography to generate a cyclonic structure called the Bonifacio gyre. Fig. 14 shows the altimetric Sea Level Anomaly obtained averaging the maps available for the 5th and 12th December 2001 (Fig. 14a), as well as the corresponding absolute altimetric sea level maps computed using the first guess (Fig. 14b) and the SMDT (Fig. 14c). The dynamic heights computed in the area relative to 500, 1000 and 1500 m are superimposed on the three plots respectively as squares, circles and triangles (for each reference depth, the mean of the dynamic heights is readjusted to the SMDT mean). In all three cases, the Bonifacio gyre is clearly visible. However, when considering only the altimetric Sea

Table 1

Comparison results: root mean square differences (RMS) in cm and regression slope (Rs) between in-situ dynamic heights measured during the NORBAL experiment and referenced to various depths and the corresponding absolute altimetric heights obtained adding to the altimetric anomalies either the SMDT, or the first guess (FG) or a zero mean (0-mean)

Depth (m)	500 m		1000 m		1500 m		2000 m	
Variance	6.6 cm		8.1 cm		8.2 cm		8.3 cm	
RMS/Rs	RMS	Rs	RMS	Rs	RMS	Rs	RMS	Rs
SMDT	2.98 (45.1)	1.11	3.30 (40.7)	1.07	3.27 (39.9)	1.08	3.40 (41.0)	1.08
FG	3.26 (49.4)	1.24	4.18 (51.6)	1.15	4.20 (51.2)	1.16	4.30 (51.8)	1.13
0-mean	3.70 (56.0)	0.96	4.16 (51.3)	0.92	4.20 (51.2)	0.91	4.40 (53.0)	0.90

In the SMDT raw, values in brackets indicate the RMS difference in percentage of variance. The second raw gives variance values computed from altimetric anomalies.

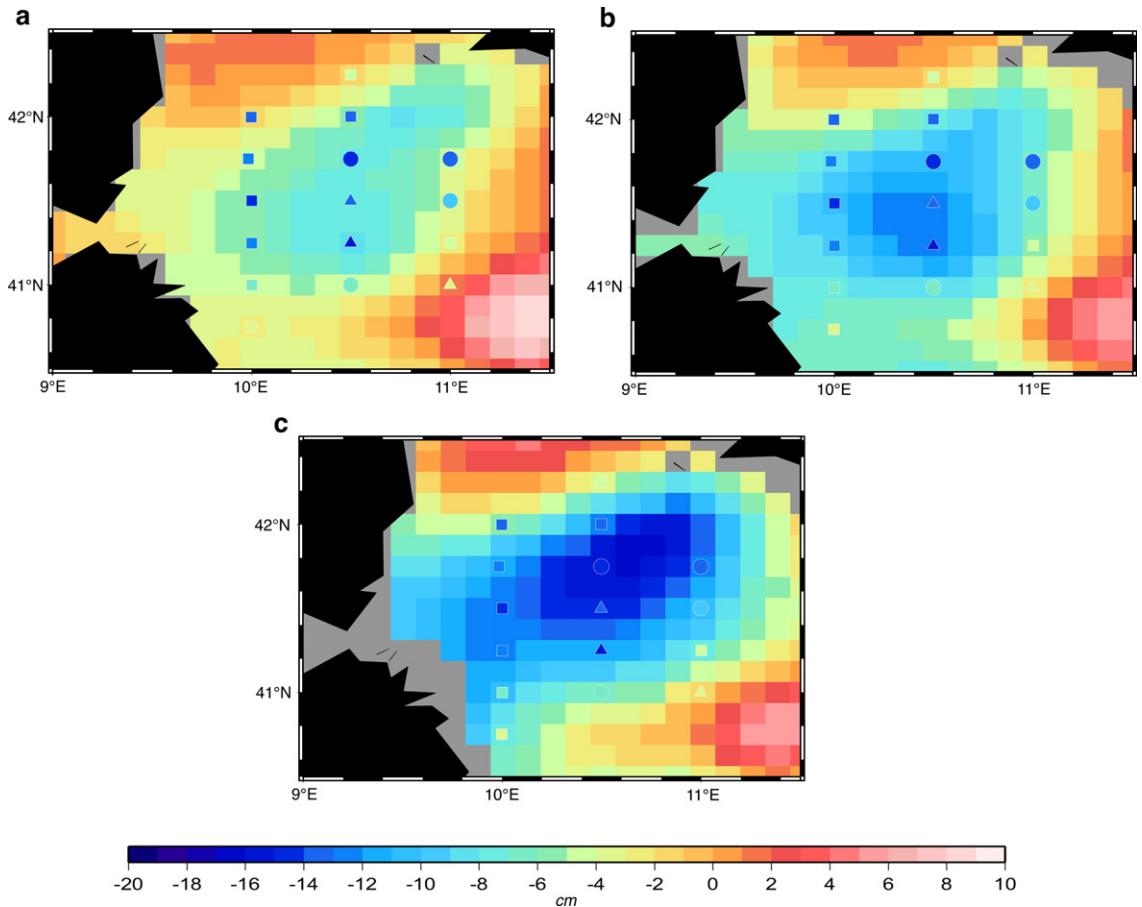


Fig. 14. Absolute altimetric height in the Bonifacio gyre area, for the period 5th to 12th December 2001, computed using to reference the altimetric anomalies a—a zero mean field b—the first guess c—the SMDT. In-situ dynamic heights measured in the area are superimposed as squares if computed relative to 500 m, as circles relative to 1000 m and as triangles relative to 1500 m.

Level Anomaly (Fig. 14a) the gyre intensity is underestimated. The use of the first guess to compute absolute altimetric level allows to increase the gyre intensity (Fig. 14b) but the core of the structure is still 5–6 cm higher than obtained by in-situ measurements. The use of the SMDT to reference altimetric anomalies clearly allows to better reproduce the position and intensity of the gyre (Fig. 14c). Consequently, the root mean square differences to all 16 dynamic heights reference to 500 m is reduced from 3.74 cm in case a (no mean is added to the altimetric anomaly) and 4.03 cm in case b (the first guess is used) to 3.64 cm in case c (the SMDT is used).

4.2.3. The Sicily channel

We used dynamic heights measured during the SYMPLEX campaign (Sicily channel—April, May 1996). A total of 329 profiles down to 400 m were available (see profile location as black dots on Fig. 15). Absolute altimetric heights compare much better to in-situ

dynamic heights when using the SMDT to reference altimetric anomalies than when using the first guess: the regression slope comes closer to one (0.96 instead of 0.88) and the root mean square difference between the two datasets is reduced (4.6 cm instead of 5.1 cm).

4.2.4. The Southern Adriatic

More surface drifting buoys have been deployed in the Adriatic from September 2002 to June 2003 as part of the DOLCEVITA program (Lee et al., 2005). The data (nearly 6400 velocity measurements) were processed as described in 2.2.1. No Ekman component was removed. As these velocity measurements were not included in the computation of the SMDT, they can be used as independent observations for validation. Absolute altimetric velocities at the time and position of the drifting buoy measurements are computed using either the SMDT or the first guess to reference altimetric anomalies (the altimetric anomalies used in this

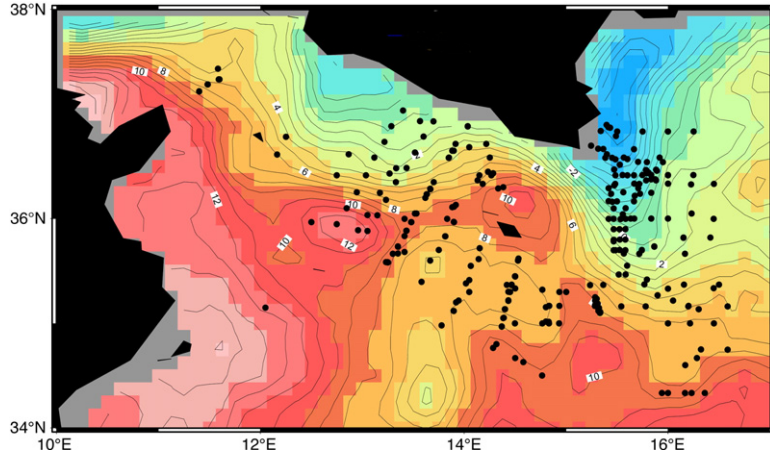


Fig. 15. The SMDT in the Sicily channel area. The color scale is the same as for Fig. 10. Contours are every centimetre. The positions of the in-situ profiles measured during the SYMPLEX campaign are indicated as black dots.

computation were obtained combining data from four different satellites—see 2.2.1) and are then compared to the in-situ velocities. When using the SMDT, the RMS difference between the altimetric absolute velocities and

the drifting buoy velocities is found equal to 9.5 cm/s for the zonal component and 11.5 cm/s for the meridional component. This constitutes an improvement in respect to the use of the first guess (10.4 cm/s and 12.6 cm/s

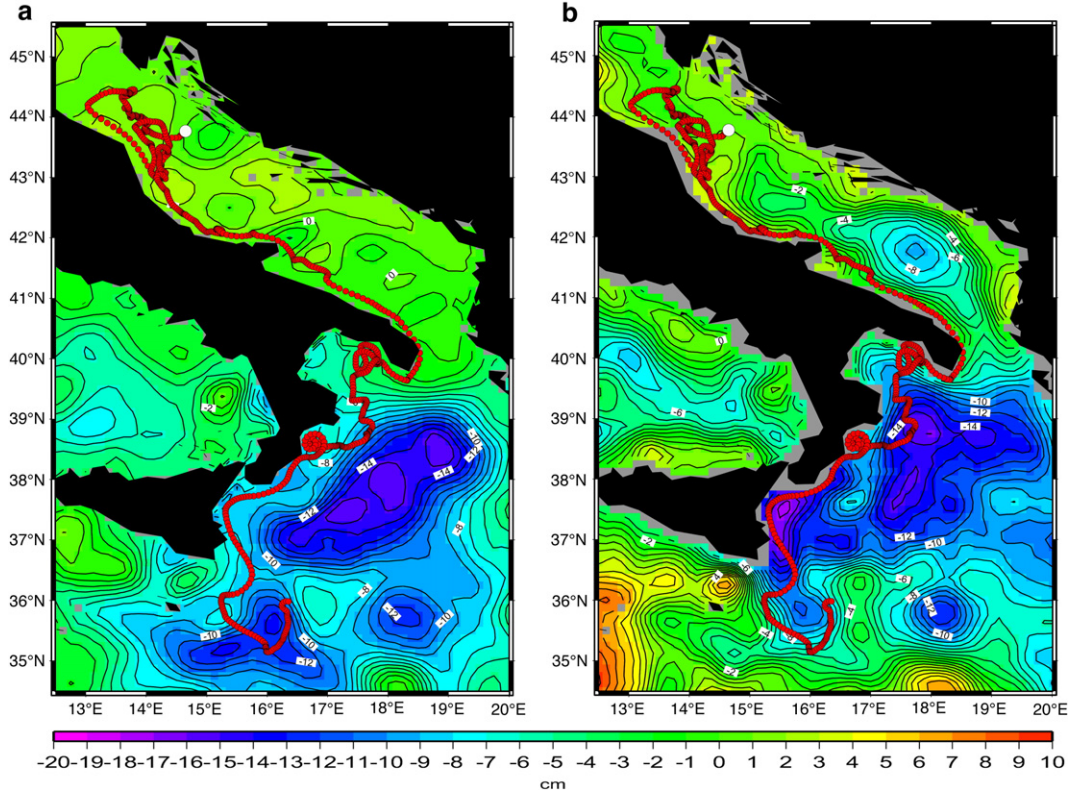


Fig. 16. Absolute altimetric sea level computed using a—a zero mean field b—the SMDT and averaged over the period December 2002–June 2003. Contours are every cm. The trajectory of the buoy b377110 is superimposed as red circles separated by 6 h. The white circle corresponds to the first position for the period considered. (For interpretation of the references to color in this figure legend, the reader is referred to the web version of this article.)

respectively for the zonal and meridional components) or a zero mean field (10.9 cm/s for the zonal component and 13.5 cm/s for the meridional component).

We present Fig. 16 the case of a drifting buoy (b37710) that was released in the Northern Adriatic on November 27th 2002. We analyse the consistency between the buoy trajectory from its release date to 30th June 2003 and the mean dynamic height, over this seven months period, measured from altimetry. Fig. 16a, where no mean was added to the altimetric Sea Level Anomalies, is compared to Fig. 16b, where the SMDT was used to compute absolute altimetric heights. In the whole Adriatic Sea, the differences between the two altimetric maps are strong: The altimetric Sea Level Anomalies are very weak (Fig. 16a) and no correspondence exists with the buoy trajectory. On the contrary, it is clearly visible on the absolute altimetric map (Fig. 16b) that the buoy was trapped after some days into the coastal current along the Italian coast and exited the Adriatic Sea through the Otranto channel. After entering the Ionian Sea it kept on flowing along the Italian coast. South of 38°N the trajectory presents two cyclonic meanders that are very well correlated with cyclonic structures visible on the absolute altimetric map, the first one centered at 15.7°E, 37.5°N and the second one centered at 15.9°E, 35.8°N. This last structure was shown to be resolved in the four satellite configuration used here but not if using altimetric data from only two satellites (Pascual et al., 2007-this issue). However, even in a four satellite configuration, the altimetric maps (also the weekly maps, not shown) fail at resolving the two small eddies (centered at 17.7°E,

40.2°N and on 16.8°E, 38.6°N) in which the buoy is clearly trapped for some days (21 days for the first one and 16 days for the second one). This might be due to the poorer precision of altimetry near the coasts.

Fig. 17 presents the maps of absolute altimetric sea level computed in the Southern Adriatic Sea using either the first guess (Fig. 17a) or the SMDT (Fig. 17b) and averaged over November 2002 as well as the trajectory from buoy b37668. In both cases, the area is characterized by an intense cyclonic gyre and, on average in November, the buoy trajectory closely follows the cyclonic path of the structure. However, in Fig. 17a, the cyclonic gyre is stretched along a northwest–southeast axis from 16.2°E, 42.5°N to 18.8°E, 40.8°N and east from 17.5°E, the buoy trajectory crosses the dynamic height isocontours toward the center of the gyre. When the SMDT is used to reference altimetric anomalies (Fig. 17b) the gyre is weaker and confined more north of the area so that the buoy trajectory follows more closely the cyclonic path around the structure. Fig. 18 shows the situation for the two following months (only the absolute maps computed using the SMDT are shown). In December (Fig. 18a) the buoy closes its tour around the gyre and is then accelerated from 41°N south to 40.2°N into the Otranto channel where it is once again trapped into a smaller cyclonic eddy so that it follows a path northward back into the Adriatic Sea. In the last days of December and the beginning of January (Fig. 18b), the buoy trajectory is slightly anticyclonic around a very coastal anticyclonic structure centered at 19.3°E, 41°N present in all altimetric maps using the SMDT from November 2002 to January 2003 but absent

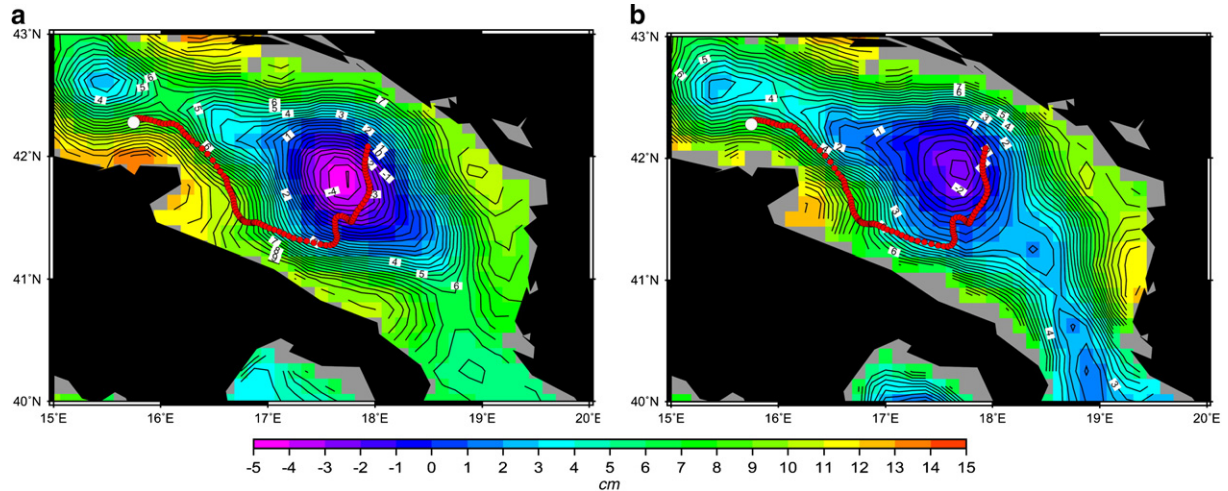


Fig. 17. Absolute altimetric sea level computed using a—the first guess mean field, b—the SMDT and averaged over November 2002. Contours are every 0.5 cm. The trajectory of the buoy b37668 is superimposed as red circles separated by 6 h. The white circle corresponds to the first position for the period considered. (For interpretation of the references to color in this figure legend, the reader is referred to the web version of this article.)

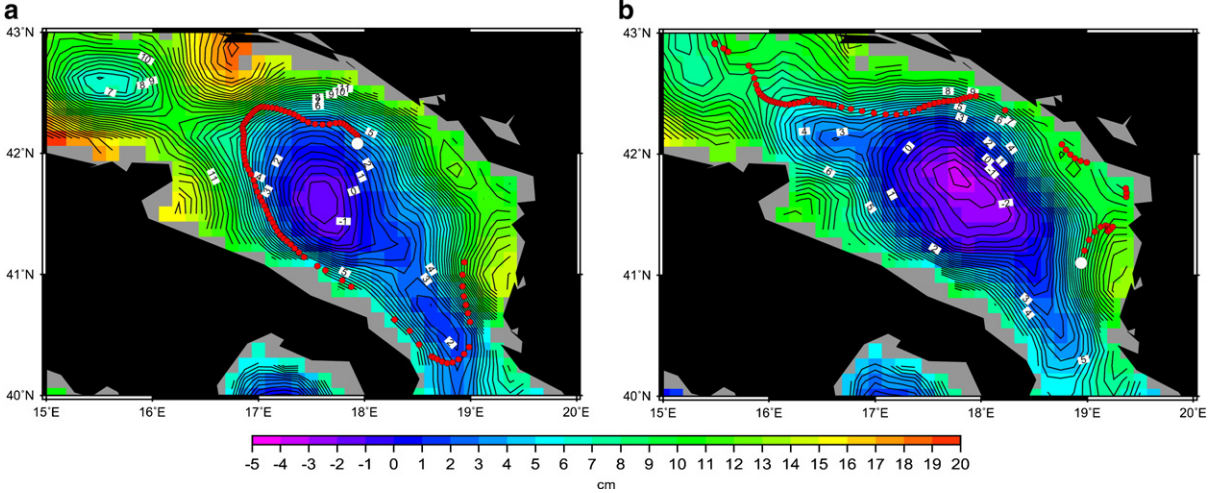


Fig. 18. Absolute altimetric sea level computed using the SMDT and averaged over a—December 2002 and b—January 2003. Contours are every 0.5 cm. The trajectory of the buoy b37668 is superimposed as red circles separated by 6 h. The white circle corresponds to the first position for the period considered. (For interpretation of the references to color in this figure legend, the reader is referred to the web version of this article.)

from the maps using the first guess (Fig. 17a, the corresponding maps for December and January are not shown). The trajectory is then north-westward along the Albanian coast, then once again cyclonic around the central cyclonic gyre and finally the buoy seems to be trapped in a current directed north-westward toward the central Adriatic Sea.

5. Illustration

In this last part, we focus on two examples highlighting the importance of using an accurate Mean Dynamic Topography to reference altimetric data in order to correctly interpret the altimetric signal. The first example is given in the Algerian Current (5.1) and the second one in the Alboran Sea (5.2).

5.1. The Algerian Current

Fig. 19 shows the evolution, during four consecutive weeks, of the Algerian Current, at its eastern part, just before the Sardaigna channel comparing, on the left side, the maps of altimetric Sea Level Anomalies and, on the right side, the corresponding maps of absolute altimetric height computed using the SMDT. The area is characterized by the formation of anticyclonic eddies, detaching from the meandering Algerian Current (see paragraph 3.1). On April, 16th 2003, the Sea Level Anomaly map features a strong cyclonic structure in the center of the area combined to an anticyclonic structure just west of Sardinia. One week later, on April, 23rd, the Sea Level Anomaly map features a stretch toward east

of the central cyclonic structure and a split into two smaller pieces of the eastern anticyclone. A much clearer view of the situation is obtained on the absolute altimetric maps, with an intense Algerian Current propagating along the African coasts, and a large anticyclonic meander steering north just west of Sardinia on April 16th. On the same day, two other anticyclonic meander of the main current, much smaller, are visible. One is centered at 6.5E and 38N and only the eastern extremity of the second one is visible, at the western side of the area. The central part of the area is occupied by small cyclonic eddies and an anticyclonic eddy centered at 5.5E and 39N. On April 23rd, the absolute altimetric map clearly indicates that the main meander has detached from the main current (centered at 7.5 E and 39N). The two smaller meanders have also detached and merged with the central anticyclonic eddy to form a more complex central anticyclonic structure. On April 30th and May 7th, the Algerian Current path remains stable on the altimetric absolute maps and the detached anticyclonic eddy slightly intensifies and propagates westward (April 30th) before merging with the more central anticyclonic structure (May 7th).

5.2. The Alboran Sea

As entering the Mediterranean Sea through the strait of Gibraltar, the Atlantic waters are known to produce two anticyclonic meanders in the Alboran Sea coupled with two anticyclonic eddies, the Western Alboran Gyre (WAG) and the Eastern Alboran Gyre (EAG). Both eddies, centered respectively on -4.5°E and -2°E

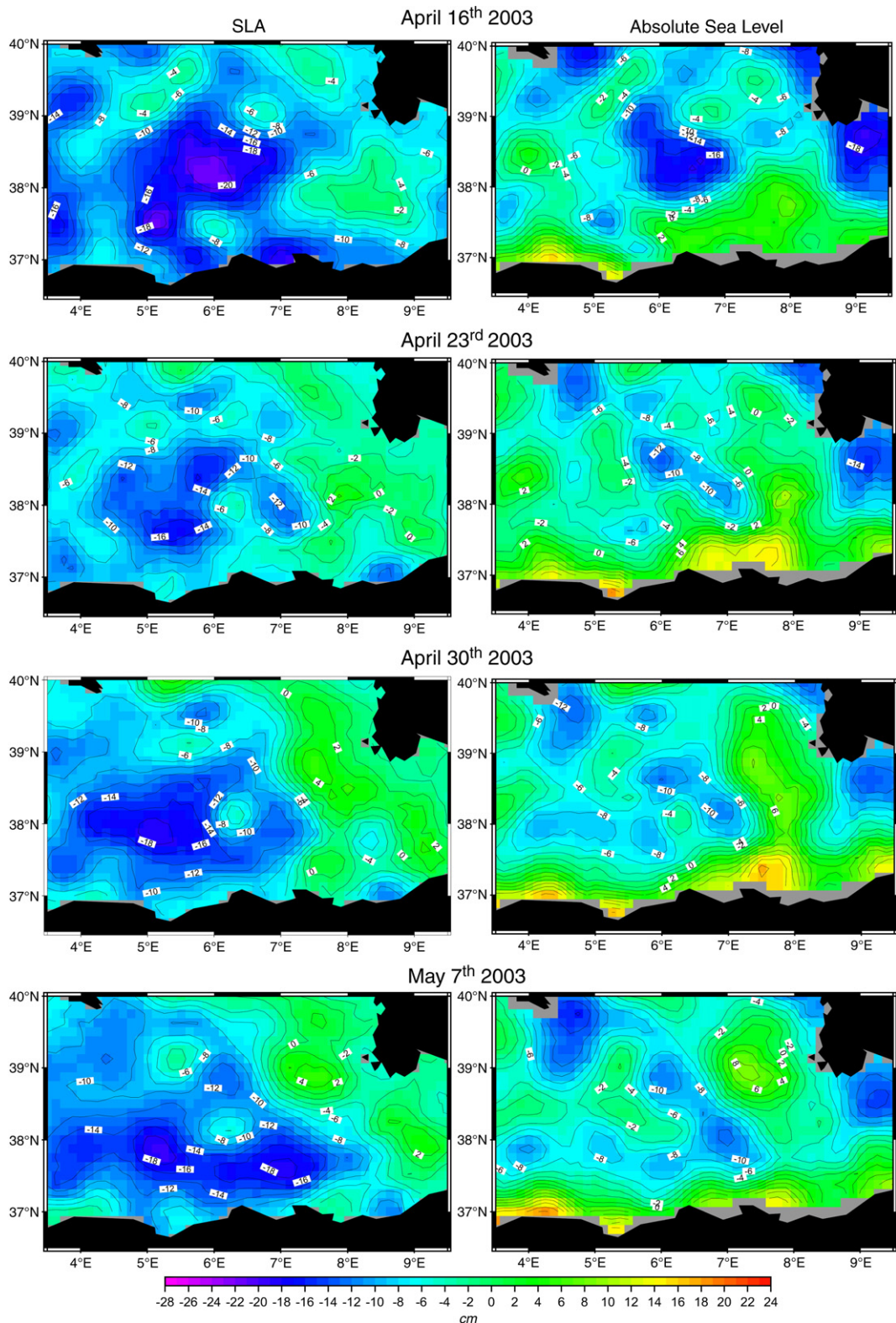


Fig. 19. Maps of altimetric anomalies (left) and absolute altimetric signal (right) in the Algerian Current from April 16th 2003 to May 7th 2003.

(Viudez et al., 1996) feature a strong inter seasonal and inter annual variability which was studied from 8 years of altimetric data by Larnicol et al. (2002). As they were missing the Mean Dynamic Topography, they inter-

preted the altimetric Sea Level Anomaly hypothesizing that the location of the gyres would not change all through the considered period so that a negative altimetric anomaly would correspond to a weakening

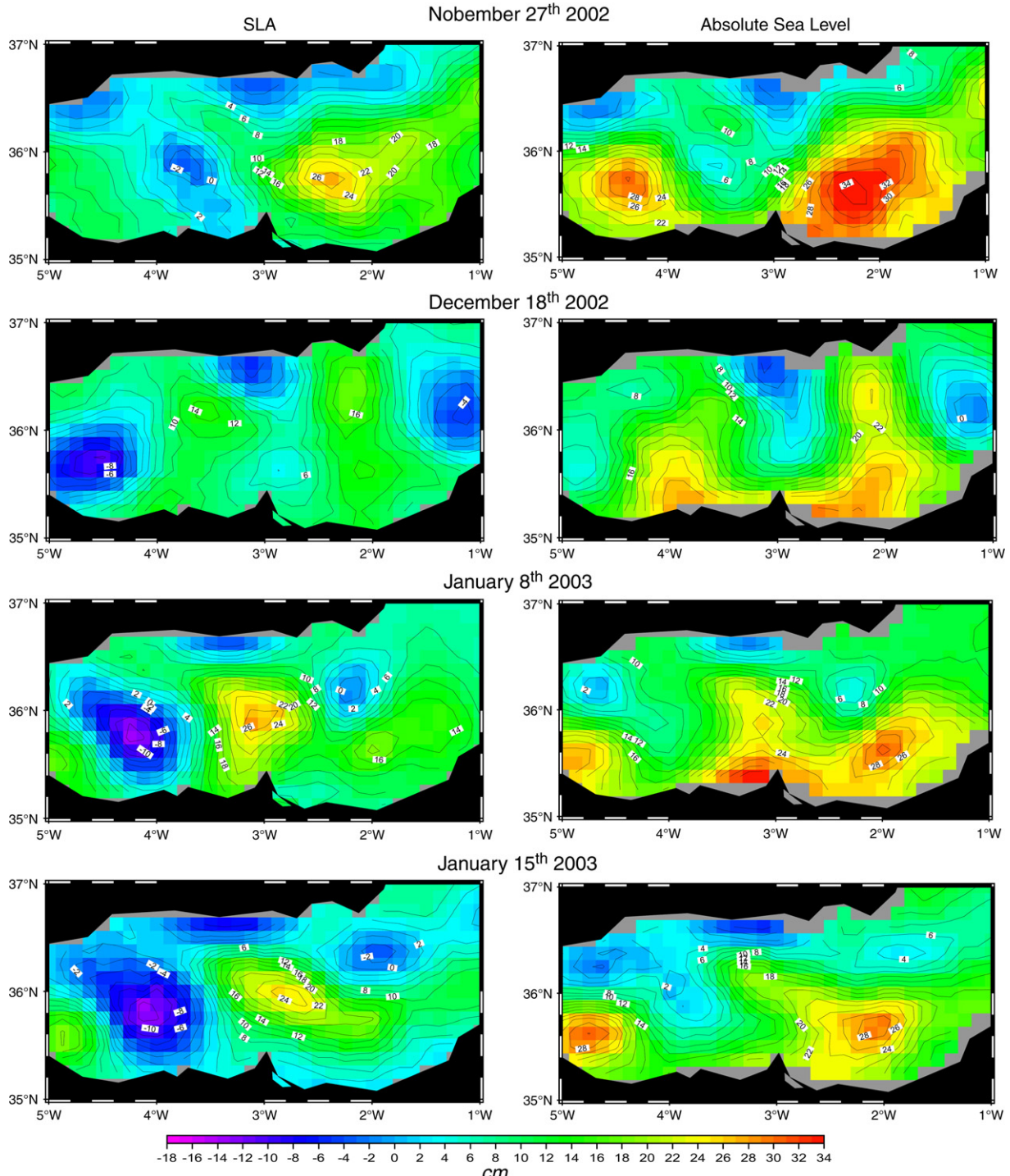


Fig. 20. Maps of altimetric anomalies (left) and absolute altimetric signal (right) in the Alboran Sea from November 27th 2002 to January 15th 2003.

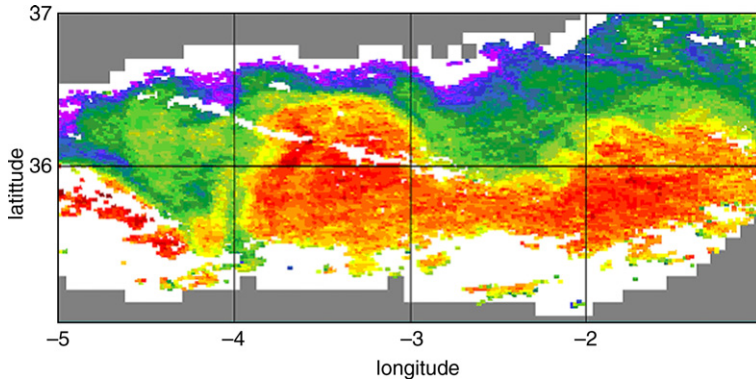


Fig. 21. SST image obtained from NOAA16-17 AVHRR sensors on January 8th 2003 in the Alboran Sea. Temperature values increase from purple to red. (For interpretation of the references to color in this figure legend, the reader is referred to the web version of this article.)

of the gyre while a positive altimetric anomaly would correspond to an intensification of the gyre. The use of the synthetic Mean Dynamic Topography to compute absolute altimetric sea level allows to highlight a more complex situation in which both gyres change in shape, strength and position from one week to the other. Fig. 20 shows the evolution of the gyres from November 27th 2002 to January 15th 2003 as seen from the altimetric anomaly maps (on the left) and the absolute altimetric maps (on the right). All through the considered period (apart on December 18th), the anomaly maps feature a cyclonic structure on the western side of the Alboran Sea, coupled with an anticyclonic structure on the eastern side, both structures changing slightly in shape and position. On November 27th, the absolute altimetric map clearly features a large meandering current all through the Alboran Sea, with two anticyclonic gyres, centered at -4.4°E and -2.2°E (respectively the WAG and the EAG). On the following absolute map given here, two weeks later, the two gyres have weakened and only their northern part remain visible. The negative signal visible on the anomaly map, centered at 4.5°E is not representative of a weakening of the gyre but, as clearly visible on the absolute map, of an eastward displacement of the WAG (centered at -4°E). The Eastern gyre has been stretched toward North and a gyre is now visible centered at -2°E , 36.3°N . On January 8th, the WAG has moved further east (centered at 3°E), the EAG is still visible on -2°E and a new meander has formed at the western extremity of the area (centered at -4.8°E). Consequently, on that day, three simultaneous anticyclonic gyres are present in the Alboran Sea. Such a situation has already been mentioned by Vargas et al. (1999) and is in very good agreement with what can be seen on a SST image obtained on the same day from NOAA16-17 AVHRR data (Fig. 21). On the successive

map (Fig. 20, January 15th 2003) the situation has turned to a more classical view of the Alboran Sea, with two anticyclonic gyres, the western one centered at -4.8°E , the second one on -2°E .

The previous examples clearly highlight the crucial importance of knowing accurately the Mean Dynamic Topography to correctly interpret the altimetric signal. The access to absolute altimetric maps allows to distinguish between a fully developed eddy and a current meander, the formation of a cyclone and the displacement of an anticyclonic structure, to follow the formation, propagation and merging of eddies. These two examples also demonstrate, though very qualitatively, the importance of the mean field if altimetric anomalies have to be assimilated into ocean circulation models: only if the mean is accurately known the altimetric data will bring into the model a pertinent information regarding the formation, propagation and dissipation of an eddy, the position of a main current, the formation of current meanders.

6. Conclusion

A Mean Dynamic Topography of the Mediterranean Sea (and the corresponding mean geostrophic circulation) was computed for the period 1993–1999 by combining in-situ drifting buoy velocities and altimetric measurements. The goal of this study was not to produce a general circulation scheme of the Mediterranean Sea since we think that the permanent/transient/recurrent character of the most known Mediterranean structures can be discussed only from the analysis of the absolute Mediterranean circulation over several decades. Altimetric data are potentially a very powerful tool for that purpose although until now, only the variable part of the signal has been exploited. In that context, the scope of

this work was to produce for the first time an estimate of the Mediterranean Mean Dynamic Topography to be used to reference altimetric Sea Level Anomalies and compute maps of absolute dynamic heights and corresponding geostrophic velocities. The method used was similar to the one described and applied for the global ocean by Rio and Hernandez (2004). The ocean variability as measured from altimetry was used to remove the variable part of the full dynamical signal as measured by drifting buoys. Doing this, synthetic estimates of the mean geostrophic circulation were obtained. In a second step, these estimates were used to correct a first guess of the Mediterranean MDT through a multivariate objective analysis. The first guess used was the mean over the period 1993–1999 of the MFSTEP modelled dynamic topography. The Synthetic Mean Dynamic Topography obtained was validated using independent in-situ measurements (hydrological profiles and drifting buoy velocities). Moreover, the importance of adding a realistic mean to altimetric anomalies in order to recover the absolute dynamical signal was illustrated. The interpretation of the altimetric measurements is considerably enhanced.

The SMDT obtained in this work can still be improved. At the present time, the method suffers from two major limitations. The first one is the different sampling capability of the datasets (drifting buoy and altimetry measurements) used to compute synthetic estimates of the mean field. The merging of altimetry data from more satellites (more than two) should help (Pascual et al., 2007-this issue). The second limitation is the number of in-situ measurements available in the Mediterranean Sea. In this study, some areas were not sampled at all by our dataset. Strong improvements should be obtained integrating more drifting buoy velocities (from 1999 until today). Also, information from in-situ hydrological profiles is potentially useful although the integration of dynamic heights is made difficult due to the unknown reference level. To make up for this difficulty, the use of recently deployed ARGO profile would be very fruitful. Finally, the information given by local accurate geoids in term of Mean Dynamic Topography could be useful in order to obtain a more precise mean in local areas. For instance, we plan to analyse the contribution of a very precise geoid computed south of the island of Crete in the framework of the GAVDOS project (Andritsanos et al., 2001).

The major application of retrieving absolute dynamic signal from altimetry is the assimilation of absolute altimetric data into general circulation models. This is crucial in the framework of developing operational forecasting systems. For instance, the integration of the

SMDT computed and described in this paper into the MFSTEP system should be tested shortly. Integrating into the system a realistic mean field of the circulation should significantly enhance its modelling and forecasting capabilities.

Finally, the accurate estimate of the Mediterranean MDT from in-situ measurements and altimetric data offers an unique opportunity for the validation of future GOCE (Gravity Field and Steady-State Ocean Circulation Explorer) data. In addition, it will be complementary to the Mean Dynamic Topography directly deduced from GOCE geoid whose limits will be precisely in areas like the Mediterranean Sea, where mean spatial scales are expected to be less than 100 km (Drinkwater et al., 2003).

Acknowledgements

We thank Nadia Pinardi and Claudia Fratantoni from INGV, Bologna, who provided the MFSTEP model fields. The NORBAL and SYMPLEX campaigns realized by ISAC-CNR were financed by the Italian Spatial Agency under contract I/R/179/02. Marie-Hélène RIO was supported by an ESA fellowship grant.

This research was partially funded by the European Commission (V Framework Program – Energy, Environment and Sustainable Development) as part of the MFSTEP project (contract number EVK-CT-2002-0007). We wish to thank all the people who made their drifter data available and who helped with drifter-related logistics and data processing.

References

- Andritsanos, V.D., Vergos, G.S., Tziavos, I.N., Pavlis, E.C., Mertikas, S.P., 2001. A high resolution geoid for the establishment of the GAVDOS multi-satellite calibration site. In: Symposia, I.A.O.G. (Ed.), Gravity Geoid and Geodynamics 2000. Springer-Verlag, Berlin Heidelberg, pp. 347–354.
- Artale, V., Astraldi, M., Buffoni, G., Gasparini, G.P., 1994. Seasonal variability of gyre-scale circulation in the North Tyrrhenian sea. *Journal of Geophysical Research* 99, 14127–14137.
- Artegiani, A., et al., 1997. The Adriatic Sea general circulation. Part II: baroclinic circulation structure. *Journal of Physical Oceanography* 27, 1515–1532.
- Ayoub, N., Le Traon, P.-Y., De Mey, P., 1998. A description of the Mediterranean surface variable circulation from combined ERS-1 and TOPEX/POSEIDON altimetric data. *Journal of Marine Systems* 18, 3–40.
- Bretherton, F.P., Davis, R.E., Fandry, C.B., 1976. A technique for objective analysis and design of oceanographic experiments applied to MODE-73. *Deep-Sea Research* 23, 559–582.
- Buongiorno Nardelli, B., Sparnocchia, S., Santoleri, R., 2001. Small mesoscale features at a meandering upper ocean front in the western Ionian Sea (Mediterranean Sea): vertical motion and potential vorticity analysis. *Journal of Physical Oceanography* 31 (8), 2227–2250.

- Davies, P., Folkard, A., Chabert d'Hières, G., 1993. Remote sensing observations of filament formation along the Almeria-Oran front. *Annals of Geophysicae* 11, 419–430.
- Davis, R.E., 1998. Preliminary results from directly measuring middepth circulation in the tropical and South Pacific. *Journal of Geophysical Research* 103 (C11), 24619–24639.
- Demirov, E., et al., 2003. Assimilation scheme of the Mediterranean Forecasting System: operational implementation. *Annals of Geophysicae* 21, 189–204.
- Drinkwater, M.R., Floberghagen, R., Haagmans, R., Muñiz, D., Popescu, A., 2003. GOCE: ESA's first Earth Explorer Core mission. In: Beutler, G.B., Drinkwater, M.R., Rummel, R., von Steiger, R. (Eds.), *Earth Gravity Field from Space—from Sensors to Earth Sciences*. Kluwer Academic Publishers, Dordrecht, Netherlands.
- Font, J., Millot, C., Salas, A.J., Chic, O., 1998. The drift of the MAW from the Alboran Sea to the Eastern Mediterranean. *Scientia Marina* 62 (3), 211–216.
- Hamad, N., Millot, C., Taupier-Letage, I., 2005. A new hypothesis about the surface circulation in the eastern basin of the Mediterranean sea. *Progress in Oceanography* 66 (2–4), 287–298.
- Hansen, D., Poulain, P.-M., 1996. Quality control and interpolations of WOCE-TOGA drifter data. *Journal of Atmospheric and Oceanic Technology* 13, 900–909.
- Iudicone, D., Santoleri, R., Marullo, S., Gerosa, P., 1998. Sea level variability and surface eddy statistics in the Mediterranean sea from TOPEX/POSEIDON data. *Journal of Geophysical Research* 103 (C2), 2995–3011.
- Lacombe, H., Tchernia, P., 1972. Caractères hydrologiques et circulation des eaux en Méditerranée. In: D.S. (Ed.), *Mediterranean Sea*. Dowden, Hutchinson & Ross, Stroudsburg, pp. 25–36.
- Larnicol, G., Le Traon, P.-Y., Ayoub, N., De Mey, P., 1995. Mean sea level and surface circulation variability of Mediterranean sea from 2 years of TOPEX/POSEIDON altimetry. *Journal of Geophysical Research* 100, 25163–25177.
- Larnicol, G., Ayoub, N., Le Traon, P.-Y., 2002. Major changes in Mediterranean Sea level variability from 7 years of TOPEX/POSEIDON and ERS-1/2 data. *Journal of Marine Systems* 33–34, 63–89.
- Le Provost, C., et al., 1999. Impact of GOCE for ocean circulation studies. Final Report n° 13175/98/NL/GD, édité par ESA Study Contract 13175/98/NL/GD.
- Le Traon, P.-Y., Dibarboure, G., 1999. Mesoscale mapping capabilities from multiple altimeter missions. *Journal of Atmospheric and Oceanic Technology* 16, 1208–1223.
- Le Traon, P.-Y., Hernandez, F., 1992. Mapping of the oceanic mesoscale circulation: validation of satellite altimetry using surface drifters. *Journal of Atmospheric and Oceanic Technology* 9, 687–698.
- Le Traon, P.-Y., Ogor, F., 1998. ERS-1/2 orbit improvement using TOPEX/POSEIDON: the 2 cm challenge. *Journal of Geophysical Research, (oceans)* 103, 8045–8057.
- Le Traon, P.-Y., Nadal, F., Ducet, N., 1998. An improved mapping method of multisatellite altimeter data. *Journal of Atmospheric and Oceanic Technology* 15, 522–533.
- Le Traon, P.-Y., Hernandez, F., Rio, M.-H., Davidson, F., 2002. How operational oceanography can benefit from dynamic topography estimates as derived from altimetry and improved geoid. In: von Steiger, R. (Ed.), *ISSI Workshop. Earth Gravity Field from Space—from Sensors to Earth Sciences. Space and Science Reviews*. Kluwer Academic Publisher, Bern, Switzerland, pp. 239–249.
- Le Vourch, J., Millot, C., Castagné, N., Le Borgne, P., Olry, J.P., 1992. *Atlas of Thermal Fronts of the Mediterranean Sea Derived from Satellite Imagery*. Mémoires de l'Institut Océanographique, Monaco.
- Lee, C.M., Askari, J., Book, S., Carniel, B., Cushman-Roisin, C., Dorman, J., Doyle, P., Flament, C., Harris, C.K., Jones, B.H., Kuzmic, M., Martin, P., Ogston, M., Perkins, H., Poulain, P.-M., Pullen, J., Russo, A., Sherwood, C., Signell, R., Detweiler, T., 2005. Northern Adriatic Response to a Wintertime Bora Wind Event. *Eos Trans. AGU* 86 (16), 157.
- Lermusiaux, P.F.J., 1999. Estimation and study of mesoscale variability in the Strait of Sicily. *Dynamics of Atmospheres and Oceans* 29, 255–303.
- Lermusiaux, P.F.J., Robinson, A.R., 2001. Features of dominant mesoscale variability, circulation patterns and dynamics in the Strait of Sicily. *Deep-Sea Research. Part 1. Oceanographic Research Papers* 48, 1953–1997.
- Manca, B., Crise, A., Scarazzato, P., Ursella, L., 2002. The response of the upper, intermediate and deep thermohaline circulation in the Ionian Sea to the temporal evolution of the Eastern Mediterranean transient. 2nd Int. Conf. on "Oceanography of the Eastern Mediterranean and Black Sea", Ankara.
- Mauerhan, T.A., 2000. Drifter Observations of the Mediterranean Sea Surface Circulation. Master of Science in Physical Oceanography Thesis, Naval Postgraduate school, Monterey, CA, 111 pp.
- Mauri, E., Poulain, P.M., 2004. Wind-driven currents in Mediterranean drifter data – MFSTEP. Internal report 1/2004/OGA/1. OGS, Trieste, Italy. 25 pp.
- Millot, C., 1985. Some features of the Algerian Current. *Journal of Geophysical Research* 90 (C4), 7169–7176.
- Millot, C., 1991. Mesoscale and seasonal variabilities of the circulation in the Western Mediterranean. *Dynamics of Atmospheres and Oceans* 15, 179–214.
- Millot, C., 1999. Circulation in the Western Mediterranean Sea. *Journal of Marine Systems* 20, 423–442.
- Nielsen, J.N., 1912. Hydrography of the Mediterranean and adjacent waters. *Rep. Dan. Oceanogr. Exp. Medit.*, vol. 1, pp. 77–192.
- Niiler, P., Maximenko, N.A., McWilliams, J.C., 2003. Dynamically balanced absolute sea level of the global ocean derived from near-surface velocity observations. *Geophysical Research Letters* 30 (22), 2164–2167.
- Ovchinnikov, I.M., 1966. Circulation in the surface and intermediate layers of the Mediterranean. *Oceanology* 6, 48–59.
- Pascual, A., Pujol, M.-I., Larnicol, G., Le Traon, P.-Y., Rio, M.-H., 2007. Mesoscale Mapping Capabilities of Multisatellite Altimeter Missions: First Results with Real Data in the Mediterranean Sea. *Journal of Marine Systems* 65, 190–211 (this issue).
- Poulain, P.-M., 1998. Lagrangian measurements of surface circulation in the Adriatic and Ionian seas between November 1994 and March 1997. *Rapp. Comm. int. Mer Medit.* 35, 190–191.
- Poulain, P.-M., 2001. Adriatic Sea Surface Circulation as derived from drifter data between 1990 and 1999. *Journal of Marine Systems* 29, 3–32.
- Poulain, P.-M., in preparation. Variability of the Ionian near-surface circulation in the 1990's as measured by Lagrangian drifters. *Deep-Sea Research*.
- Poulain, P.-M., Zambianchi, E., in press. Surface circulation in the central Mediterranean Sea as deduced from Lagrangian drifters in the 1990's. *Cont. Shelf Res.*
- Poulain, P.-M., Barbanti, R., Cecco, R., Fayos, C., Mauri, E., Ursella, L., Zanasca, P., 2004. Mediterranean Surface Drifter Database: 2 June 1986 to 11 November 1999. Tech. Rep. 78/2004/OGA/31. OGS, Trieste, Italy. CD-ROM and online dataset http://poseidon.ogs.trieste.it/drifter/database_med.
- Pujol, M.I., Larnicol, G., 2005. Mediterranean Sea eddy kinetic energy variability from 11 years of altimetric data. *Journal of Marine Systems* 58 (3–4), 121–142.

- Rio, M.-H., Hernandez, F., 2004. A Mean Dynamic Topography computed over the world ocean from altimetry, in-situ measurements and a geoid model. *Journal of Geophysical Research* 109 (12).
- Robinson, A.R., Golnaraghi, M., 1993. Circulation and dynamics of the Eastern Mediterranean Sea: quasi-synoptic data-driven simulations. *Deep-Sea Research. Part 2. Topical Studies in Oceanography* 40 (6), 1207–1246.
- Robinson, A.R., et al., 1991. The Eastern Mediterranean general circulation: features, structure and variability. *Dynamics of Atmospheres and Oceans* 15, 215–240.
- Robinson, A.R., 1999. The Atlantic Ionian stream. *Journal of Marine Research* 20, 129–156.
- Salas, J., Garcia-Ladona, E., Font, J., 2001. Statistical analysis of the surface circulation in the Algerian Current using Lagrangian buoys. *Journal of Marine Systems* 29, 69–85.
- Theocharis, A., Georgopoulos, D., Lascaratos, A., Nittis, K., 1993. Water masses and circulation in the central region of the Eastern Mediterranean: Eastern Ionian, South Aegean and Northwest Levantine, 1986–1987. *Deep-Sea Research* 40 (6), 1121–1142.
- Theocharis, A., Balopoulos, E., Kioroglou, S., Kontoyiannis, H., Iona, A., 1999. A synthesis of the circulation and hydrography of the South Aegean Sea and the straits of the Cretan Arc (March 1994–January 1995). *Progress in Oceanography* 44, 469–509.
- Tintore, J., Gomis, D., Alonso, S., Parilla, G., 1991. Mesoscale dynamics and vertical motion in the Alboran sea. *Journal of Physical Oceanography* 21 (6), 811–823.
- Tintore, J., Viudez, A., Gomis, D., Alonso, S., Werner, F., 1994. Mesoscale variability and Q vector vertical motion in the Alboran Sea. In: La Violette, P.E. (Ed.), *Seasonal and Interannual Variability of the Western Mediterranean Sea, Coastal and Estuarine Studies*, pp. 47–71.
- Vargas, M., Plaza, F., Garcia Lafuente, J., Vargas, J.M., Sarhan, T., 1999. The variability of the Alboran sea at different time and length scales. 4th Mediterranean Target Project Workshop, Perpignan, France.
- Viudez, A., Tintore, J., Haney, R.L., 1996. Circulation in the Alboran sea as determined by quasi-synoptic hydrographic observations. Part I: three-dimensional structure of the two anticyclonic gyres. *Journal of Physical Oceanography* 26, 684–705.